Bone marrow adipocytes promote the regeneration of stem cells and hematopoiesis by secreting SCF

Bo O. Zhou[1,2,7], **Hua Yu**[1], **Rui Yue**[2], **Zhiyu Zhao**[2], **Jonathan J. Rios**[3,4], **Olaia Naveiras**[5], and **Sean J. Morrison**[2,6,7]

[1]State Key Laboratory of Cell Biology, CAS Center for Excellence in Molecular Cell Science, Shanghai Institute of Biochemistry and Cell Biology, Chinese Academy of Sciences; University of Chinese Academy of Sciences, 320 Yueyang Road, Shanghai 200031, P. R. China [2]Department of Pediatrics and Children's Research Institute [3]McDermott Center for Human Growth and Development, University of Texas Southwestern Medical Center, Dallas, Texas 75390, USA [4]Texas Scottish Rite Hospital for Children, 2222 Welborn Street, Dallas, Texas, 75219, USA [5]Institute of Bioengineering, Ecole Polytechnique Fédérale de Lausanne (EPFL), Lausanne CH-1015, Switzerland [6]Howard Hughes Medical Institute

Abstract

Endothelial cells and Leptin Receptor+ (LepR+) stromal cells are critical sources of haematopoietic stem cell (HSC) niche factors, including Stem Cell Factor (SCF), in bone marrow. After irradiation or chemotherapy, these cells are depleted while adipocytes become abundant. We discovered that bone marrow adipocytes synthesize SCF. They arise from *Adipoq*-Cre/ER+ progenitors, which represent ~5% of LepR+ cells, and proliferate after irradiation. *Scf* deletion using *Adipoq*-Cre/ER inhibited hematopoietic regeneration after irradiation or 5-fluorouracil treatment, depleting HSCs and reducing mouse survival. *Scf* from LepR+ cells, but not endothelial, hematopoietic, or osteoblastic cells, also promoted regeneration. In non-irradiated mice, *Scf* deletion using *Adipoq*-Cre/ER did not affect HSC frequency in long bones, which have few adipocytes, but depleted HSCs in tail vertebrae, which have abundant adipocytes. A-ZIP/F1 'fatless" mice exhibited delayed hematopoietic regeneration in long bones but not in tail vertebrae, where adipocytes inhibited vascularization. Adipocytes are a niche component that promotes hematopoietic regeneration.

HSCs reside in a perivascular niche in the bone marrow created partly by endothelial cells and Leptin Receptor+ (LepR+) stromal cells[1,2]. Approximately 80% of dividing and non-dividing HSCs in the bone marrow are adjacent to sinusoidal blood vessels, while another 10% are near arterioles and 10% are near transition zone vessels[3]. More than 90% of the

---

[7]Co-corresponding authors: sean.morrison@utsouthwestern.edu; bo.zhou@sibcb.ac.cn.

cells that express high levels of *Scf* and *Cxcl12* in normal young adult bone marrow are LepR[+], while endothelial cells express much lower levels of *Scf* and *Cxcl12*[4]. Conditional deletion of *Scf* or *Cxcl12* from LepR^{+} cells or endothelial cells depletes HSCs[1,2,5]. Deletion of *Scf* from LepR^{+} cells and endothelial cells in the same mice eliminates all quiescent and serially-transplantable HSCs from adult bone marrow[6]. The niche cells we identified based on LepR expression have also been identified by others based on their expression of high levels of *Cxcl12*[7–9], low levels of the *Nestin*-GFP transgene[10,11], PDGFRα[4,12], and *Prx1*-Cre[5].

Skeletal stem cells (SSCs) in the bone marrow contribute to the HSC niche[10,13,14] and LepR^{+} cells include the SSCs that give rise to nearly all of the fibroblast colony-forming cells as well as most of the osteoblasts and adipocytes that form in adult bone marrow[4,15]. While restricted adipocyte progenitors have been characterized in fat depots outside of the bone marrow[16–18] the identity of adipocyte progenitors in the bone marrow remains uncertain[15,19–21]. Additional cell types, including Schwann cells[22], nerve fibers[10,23,24], macrophages[25,26] and megakaryocytes[27,28], also directly or indirectly regulate the niche.

Adipocytes are rare in the marrow of most young adult mouse bones, but dramatically increase in frequency during aging and after myeloablation[29–33]. HSC frequency is lower in tail vertebrae, where adipocytes are abundant, than in thoracic vertebrae, where adipocytes are rare[29]. Expression of the dominant negative A-ZIP/F protein under the *Fabp4* promoter[34] reduces adipogenesis in mice and increases HSC frequency in tail vertebrae, accelerating hematopoietic recovery after irradiation[29]. These data suggested that bone marrow adipocytes negatively regulate HSC function and hematopoietic recovery[29], though it remains unclear whether this reflects a direct effect on HSCs or an indirect effect on the niche. A-ZIP/F1 mice also exhibit changes in angiogenesis[35,36] and regeneration of bone marrow sinusoids is critical for hematopoietic regeneration after irradiation[37–39].

Irradiation and chemotherapy not only deplete HSCs but also disrupt their niche by destroying sinusoidal blood vessels and depleting stromal cells[37,39–41]. Niche regeneration is necessary for regeneration of HSCs and hematopoiesis[37,39]. Denervation with 6-hydroxydopamine does not alter normal hematopoiesis but significantly inhibits regeneration after irradiation[24]. Here we report that bone marrow adipocytes, but not adipocytes in peritoneal fat pads, express a high level of *Scf* and that *Scf* from these cells promotes the regeneration of HSCs and hematopoiesis after irradiation or 5-fluorouracil (5-FU) treatment. Our results also reveal differences in adipocyte function among bones as adipocytes in tail vertebrae, but not long bones, inhibit bone marrow vascularization. The net result is that adipocytes in long bones promote hematopoietic recovery after irradiation while in caudal vertebrae they inhibit hematopoietic regeneration despite being an important source of SCF in both locations.

RESULTS

Irradiation changes the bone marrow stroma

Lepr[cre]*; R26*[tdTomato] mice were irradiated and transplanted with one million bone marrow cells for radioprotection. As expected, the numbers of bone marrow cells, blood cells, and

Lineage$^-$Sca-1$^+$c-kit$^+$ (LSK) stem/progenitor cells substantially declined two weeks after irradiation but rebounded to normal or near normal levels by four weeks after irradiation (Fig. 1a–1e; Supplementary Fig. 1a–e). Consistent with prior studies[38,40], sinusoids were also reduced in number and substantially dilated two weeks after irradiation but largely recovered in number and morphology by four weeks after irradiation (Fig. 1f–i). We did not observe changes in the number or morphology of arterioles after irradiation (Fig. 1f–h and 1j). Consistent with the damage to sinusoids, the numbers of VE-cadherin$^+$ endothelial cells (Fig. 1k) and Tomato$^+$ stromal cells (Fig. 1l) declined two weeks after irradiation but then partially recovered by 4 weeks after irradiation.

In contrast to the flow cytometry data, the number of Tomato$^+$ stromal cells after irradiation did not appear markedly different than in non-irradiated controls in sections (Fig. 1f–h). This appeared to be due to the differentiation of LepR$^+$ cells into perilipin$^+$ adipocytes, which are visible in sections but are too large and fragile to detect by flow cytometry. Adipocytes are Tomato$^+$ in these mice because they derive from LepR$^+$ cells (ref[4] and Supplementary Fig. 1f). Adipocytes were rare in femurs from non-irradiated mice but became abundant two weeks after irradiation before modestly declining in number by 4 weeks after irradiation (Fig. 1m–p).

LepR$^+$ stromal cells and adipocytes are the primary sources of *Scf* after irradiation

In 2-month-old *Lepr^{cre}; R26^{tdTomato}; Scf^{GFP}* mice, *Scf*-GFP was expressed at a high level by Tomato$^+$CD45$^-$Ter119$^-$ stromal cells (Fig. 2a) and at a low level by VE-cadherin$^+$CD45$^-$Ter119$^-$ endothelial cells (Fig. 2b). Irradiation did not appear to affect the percentage of endothelial cells or LepR$^+$ cells that expressed *Scf*-GFP or the level of expression (Fig. 2a, b). Most *Scf*-GFP^{high} cells were Tomato$^+$ in the bone marrow of *Lepr^{cre}; R26^{tdTomato}; Scf^{GFP}* mice before and after irradiation (Supplementary Fig. 2a).

Tomato$^+$ cells were associated with sinusoids as well as large and small diameter arterioles throughout the bone marrow of *Lepr^{cre}; R26^{tdTomato}; Scf^{GFP}* mice (Fig. 2c). The Tomato$^+$ stromal cells around sinusoids and small diameter arterioles were uniformly positive for *Scf*-GFP (Fig. 2c, arrows). The Tomato$^+$ stromal cells around large diameter arterioles near the center of the bone marrow were negative for *Scf*-GFP (Fig. 2c, arrowheads). Two weeks after irradiation, *Scf*-GFP$^+$Tomato$^+$ stromal cells remained primarily around sinusoids and small diameter arterioles (Fig. 2d). *Scf*-GFP expression was not detected in hematopoietic cells or in osteoblasts/osteocytes of 2-month-old *Col1a1*2.3-cre; R26^{tdTomato}; Scf^{GFP}* mice, with or without irradiation (Supplementary Fig. 2b–e).

We confirmed the identity of adipocytes by staining with an antibody against perilipin, a protein that coats lipid droplets in the cytoplasm[42]. In non-irradiated 2 month-old mice, perilipin$^+$ adipocytes were rare (Fig. 1n) but always positive for *Scf*-GFP (Fig. 2e; Supplementary Fig. 3a). Although these cells derive from LepR$^+$ cells[4], perilipin$^+$ adipocytes were negative for anti-LepR antibody staining (Fig. 2g). Two weeks after irradiation, the numbers of perilipin$^+$ adipocytes in bone marrow sections increased dramatically and these cells remained *Scf*-GFP$^+$ (Fig. 2f). Note that although perilipin positive cells always stained positively for *Scf*-GFP, the staining did not overlap in all optical sections (1μm thick) because *Scf*-GFP is present throughout the cytoplasm while perilipin is

not[42]. Since adipocytes arise from LepR^{+} cells in the bone marrow, *Scf*-GFP overlapped with Tomato in perilipin[+] adipocytes in *Lepr^cre; R26^tdTomato; Scf^GFP* mice (Supplementary Fig. 2f, g).

Quantitative reverse transcription PCR (qPCR) showed that *Scf* was expressed by LepR^{+} stromal cells at high levels and in VE-cadherin^{+} endothelial cells at low levels, but not by CD45^{+}/Ter119^{+} hematopoietic cells or *Col1a1*2.3*-GFP^{+} osteoblasts, in irradiated or non-irradiated bone marrow (Fig. 2h). Since adipocytes cannot be isolated by flow cytometry, we isolated them by collecting the floating cells after enzymatic dissociation of bone marrow cells. Adipocytes from irradiated and non-irradiated bone marrow, but not from intraperitoneal fat pads, expressed *Scf* at a level comparable to LepR^{+} stromal cells (Fig. 2h). We confirmed adipocyte purity by also assessing *leptin* (a marker of adipocytes but not LepR^{+} stromal cells) and full length *Lepr* (a marker of LepR^{+} cells but not adipocytes) (Supplementary Fig. 3b and 3c). Two other adipocyte markers, *perilipin* and *FABP4*, were also abundant in adipocytes but absent from LepR^{+} stromal cells (Supplementary Fig. 3e, f). *Adiponectin* (*Adipoq*), a marker of adipocytes and their progenitors, was detected in adipocytes and at a lower level in LepR^{+} cells (Supplementary Fig. 3d).

Human bone marrow from 8 to 17 year-old donors contained large numbers of adipocytes (Supplementary Fig. 3g) and *Scf* transcripts were 52 ± 11 fold enriched in human bone marrow adipocytes as compared to bone marrow mononuclear cells (Fig. 2i).

Scf from osteoblastic, hematopoietic, and endothelial cells is not required for regeneration

We conditionally deleted *Scf* from osteoblasts using *Col1a1*2.3*-Cre[1,43] (Supplementary Fig. 2d). Non-irradiated adult *Col1a1*2.3-cre; Scf^GFP/fl* mice had normal blood cell counts and normal numbers of total bone marrow cells, LSK cells, and CD150^{+}CD48^{−}Lineage^{−}Sca-1^{+}c-kit^{+} HSCs[44] in the bone marrow (Supplementary Fig. 4a–f). Irradiated *Col1a1*2.3-cre; Scf^GFP/fl* mice transplanted with wild-type bone marrow cells also did not significantly differ from irradiated and transplanted control mice at 2 or 4 weeks after irradiation with respect to blood cell counts or numbers of total bone marrow cells, LSK cells, or HSCs in the bone marrow (Supplementary Fig. 4a–f). Bone marrow cells competitively transplanted from these *Col1a1*2.3-cre; Scf^GFP/fl* recipients at 4 weeks after irradiation gave similar levels of donor cell reconstitution in all lineages as compared to bone marrow cells from control recipients (Supplementary Fig. 4g). Therefore, *Scf* expression by osteoblasts is dispensable for hematopoietic regeneration.

Conditional deletion of *Scf* from hematopoietic cells using *Vav1*-Cre, also did not affect blood cell counts, LSK cells, or HSCs in the bone marrow or non-irradiated (Supplementary Fig. 4h–m) or irradiated mice (Supplementary Fig. 4h–m). Competitive secondary transplantation at 4 weeks after irradiation found no differences in the reconstituting capacity of *Vav1-cre; Scf^GFP/fl* versus control bone marrow cells (Supplementary Fig. 4g). *Scf* expression by hematopoietic cells is also dispensable for hematopoietic regeneration.

Non-irradiated *Tie2-cre; Scf^GFP/fl* mice had normal blood cell counts (Fig. 3a–c) but significantly fewer LSK cells, and HSCs as compared to non-irradiated control mice (Fig. 3d–f). In contrast, at 2 or 4 weeks after irradiation we observed no significant difference

between control mice reconstituted with control bone marrow cells versus *Tie2-cre; Scf*$^{GFP/fl}$ mice reconstituted by control bone marrow in terms of blood cell counts, or the numbers of total cells, LSK cells, or HSCs in the bone marrow (Fig. 3a–f). Bone marrow cells competitively transplanted from these *Tie2-cre; Scf*$^{GFP/fl}$ recipients at 4 weeks after irradiation gave similar levels of donor cell reconstitution in all lineages as compared to bone marrow cells from control recipients (Fig. 3g). Therefore, the low level of SCF produced by endothelial cells contributes to HSC maintenance and hematopoiesis in normal adult bone marrow but is dispensable for hematopoietic regeneration after irradiation.

Scf from LepR⁺ cells promotes hematopoietic regeneration

In non-irradiated bone marrow from 2 month-old *Lepr*^{cre}; *R26*^{tdTomato} mice, more than 95% of Tomato⁺ cells (Supplementary Fig. 5a, d) as well as cells that express high levels of *Scf*-GFP, stain positively with an antibody against LepR (Fig. 2g)[4]. At 2 and 4 weeks after irradiation, the accumulation of adipocytes (Fig. 1o) that derive from LepR⁺ cells (Supplementary Fig. 1f) reduced the proportion of Tomato⁺ bone marrow cells that stained positively for anti-LepR antibody as differentiation to adipocytes abolished LepR expression (Supplementary Fig. 5a–d).

Non-irradiated *Lepr*^{cre}; *Scf*$^{GFP/fl}$ mice had normal blood cell counts (Fig. 3h–3j) but significantly lower bone marrow cellularity (Fig. 3k) and numbers of LSK cells (Fig. 3l) and HSCs (Fig. 3m) as compared to non-irradiated control mice. To test whether LepR⁺ cells and their progeny promote hematopoietic regeneration after irradiation we transplanted *Lepr*^{cre}; *Scf*$^{GFP/fl}$ mice and *Scf*$^{GFP/fl}$ controls with wild-type bone marrow cells and compared hematopoietic reconstitution. *Lepr*^{cre}; *Scf*$^{GFP/fl}$ recipients had much lower levels of SCF in the bone marrow as compared to control mice at 2 weeks after irradiation (Supplementary Fig. 5e). At 2 and 4 weeks after irradiation, *Lepr*^{cre}; *Scf*$^{GFP/fl}$ mice had significantly lower white (Fig. 3h) and red blood cell counts (Fig. 3i) as well as bone marrow cellularity (Fig. 3k) and numbers of LSK cells (Fig. 3l) and HSCs (Fig. 3m) as compared to control mice. Competitive secondary transplantation of bone marrow cells from these recipient mice confirmed the significantly reduced reconstituting activity of bone marrow cells from *Lepr*^{cre}; *Scf*$^{GFP/fl}$ as compared to control recipients (Fig. 3n). Significantly more *Lepr*^{cre}; *Scf*$^{GFP/fl}$ recipients died after irradiation and transplantation of 2×10^5 bone marrow cells as compared to control recipients (Fig. 3o).

Adipoq-Cre/ER expression identifies adipocyte progenitors

Adiponectin-Cre/ER (*Adipoq*-Cre/ER), which recombines in adipocytes in white adipose depots[45,46], also recombined in bone marrow adipocytes. Four weeks after gavaging 6-week-old *Adipoq-cre/ER; R26*^{tdTomato} mice with tamoxifen, Tomato was expressed in $0.017\pm0.0008\%$ of bone marrow cells (Fig. 4a), including $93\pm5\%$ of perilipin⁺ adipocytes (Fig. 4b). Virtually all of the Tomato expression in the bone marrow outside of adipocytes was in a subset of LepR⁺ stromal cells: $5.9\pm3.1\%$ of LepR⁺ cells in *Adipoq-cre/ER; R26*^{tdTomato} bone marrow were Tomato⁺ (Fig. 4c). We did not detect Tomato expression in hematopoietic cells (Fig. 4a), VE-cadherin⁺ endothelial cells (Fig. 4b, e), or osteoblasts (Fig. 4d). Thus, *Adipoq*-Cre/ER recombines in *Scf*-GFP-expressing adipocytes in the bone marrow as well as in a small subset of LepR⁺ stromal cells (Fig. 4c, f, g).

At four weeks after tamoxifen treatment, both LepR$^+$Tomato$^+$ cells and LepR$^+$Tomato$^-$ cells from *Adipoq-cre/ER; R26^{tdTomato}* mice formed CFU-F colonies (Fig. 4h), and differentiated into oil-red O$^+$ adipocytes and Alizarin-red$^+$ osteoblasts (Fig. 4i). However, LepR$^+$Tomato$^+$ cells spontaneously formed many more perilipin$^+$ adipocytes as compared to LepR$^+$Tomato$^-$ cells (Fig. 4j; Supplementary Fig. 6a, b).

To determine the fate of *Adipoq*-Cre/ER$^+$ cells in vivo, we treated 6-week-old *Adipoq-cre/ER; R26^{tdTomato}* mice with tamoxifen then analyzed femur bone marrow 2 to 24 weeks later. Two weeks after tamoxifen, Tomato$^+$ stromal cells accounted for only 0.009±0.0004% of enzymatically dissociated bone marrow cells (Fig. 5a), including 3.5±2.3% of LepR$^+$ cells (Fig. 5b), and 95±2.3% of perilipin$^+$ adipocytes (Fig. 5c), which were rare in femur bone marrow (Fig. 5d). The percentages of bone marrow cells and LepR$^+$ cells that were Tomato$^+$, as well as the numbers of adipocytes in the bone marrow, all increased over time. By 16 weeks after tamoxifen treatment, Tomato$^+$ stromal cells accounted for 0.07±0.02% of bone marrow cells (Fig. 5a), including 23±5.9% of LepR$^+$ cells (Fig. 5b), and 78±11% of perilipin$^+$ adipocytes (Fig. 5c). In normal adult mice, *Adipoq*-Cre/ER$^+$LepR$^+$ stromal cells thus expand in number and give rise to increasing numbers of adipocytes over time (Fig. 5d). Although *Adipoq*-Cre/ER$^+$ cells had the potential to form bone in culture, they rarely formed osteoblasts in vivo (Fig. 5e, f). This suggests these cells are specified to form adipocytes in vivo.

The percentage of Tomato$^+$ adipocytes modestly declined between 2 and 24 weeks after tamoxifen treatment (Fig. 5c). This suggests that *Adipoq*-Cre/ER$^+$ adipocyte progenitors were replenished by LepR$^+$*Adipoq*-Cre/ER$^-$ SSCs as they differentiated into adipocytes.

We treated *Adipoq-cre/ER; R26^{tdTomato}* mice with tamoxifen 2 weeks before irradiation and bone marrow transplantation. Two weeks after irradiation, LepR$^+$Tomato$^+$ stromal cells and LepR$^+$Tomato$^-$ stromal cells were dramatically depleted in the bone marrow (Fig. 5g, h), partly as a result of cell death (Fig. 5i). The numbers of these cells in the bone marrow increased between 2 and 4 weeks after irradiation but remained significantly lower than in non-irradiated bone marrow (Fig. 5g, h). In contrast, the number of LepR negative adipocytes dramatically increased after irradiation (Fig. 5k).

In normal young adult mice adipocyte progenitors were quiescent (Fig. 5m). However, 2 weeks after irradiation, Tomato$^+$ adipocyte progenitors had gone into cycle (Fig. 5m and 5n). Tomato$^+$ cells from *Lepr^{cre}; R26^{tdTomato}* mice were also quiescent in normal young adult mice but went into cycle after irradiation (Fig. 5m and 5n).

Bone marrow adipocytes are an important source of *Scf*

Deletion of *Scf* with *Adipoq*-Cre/ER had little effect on SCF protein levels in non-irradiated bone marrow but substantially reduced SCF levels in irradiated bone marrow (Supplementary Fig. 5e). Non-irradiated 3-month-old *Adipoq-cre/ER; Scf$^{GFP/fl}$* mice at 4 weeks after tamoxifen administration had normal blood cell counts (Fig. 6a–c), normal bone marrow cellularity (Fig. 6d) and normal numbers of LSK cells (Fig. 6e) and HSCs (Fig. 6f) in femur and tibia bone marrow. In contrast, by 4 weeks after irradiation and transplantation of wild-type bone marrow cells, *Adipoq-cre/ER; Scf$^{GFP/fl}$* mice had significantly lower red

blood cell counts (Fig. 6b), total bone marrow cells (Fig. 6d), LSK cells (Fig. 6e), and HSCs (Fig. 6f) in their femurs and tibias as compared to irradiated $Scf^{GFP/fl}$ controls.

Bone marrow cells from the femurs and tibias of non-irradiated $Adipoq$-$cre/ER; Scf^{GFP/fl}$ mice gave similar levels of donor cell reconstitution as non-irradiated control bone marrow cells upon transplantation into irradiated mice (Fig. 6g). However, bone marrow cells from $Adipoq$-$cre/ER; Scf^{GFP/fl}$ recipient mice at 4 weeks after irradiation gave significantly lower levels of donor cell reconstitution as compared to bone marrow cells from $Scf^{GFP/fl}$ recipient mice (Fig. 6h). A significantly higher proportion of $Adipoq$-$cre/ER; Scf^{GFP/fl}$ mice died after irradiation and bone marrow transplantation as compared to control mice (Fig. 6i). Therefore, Scf from adipocytes promotes hematopoietic regeneration and mouse survival after irradiation.

Although SCF acts directly on HSCs to promote c-kit receptor signaling[47,48], Scf deletion could potentially also indirectly affect HSCs as a result of changes in stromal cells; however, few megakaryocytes or endothelial cells expressed c-kit (Supplementary Fig. 7a–d) and Scf deletion using $Adipoq$-CreER did not significantly affect the morphologies or frequencies of megakaryocytes, sinusoids, or arterioles in the bone marrow at 4 weeks after irradiation (Supplementary Fig. 7e–h).

We also induced myeloablation by treating with 5-FU. Twelve days later we observed abundant perilipin[+] adipocytes throughout the bone marrow (Supplementary Fig. 6e). $Adipoq$-$cre/ER; Scf^{GFP/fl}$ mice had significantly fewer bone marrow cells (Fig. 6j), LSK cells (Fig. 6k), and HSCs (Fig 6l; HSC markers are effective 12 days after 5-FU treatment, ref[49]) as compared to $Scf^{GFP/fl}$ control mice 12 days after 5-FU treatment. Significantly more $Adipoq$-$cre/ER; Scf^{GFP/fl}$ mice died after two doses of 5-FU as compared to control mice (Fig. 6m). SCF synthesized by adipocytes thus promotes hematopoietic regeneration after 5-FU treatment.

Scf from adipocytes promotes HSC maintenance in caudal vertebrae

Differences in the numbers of adipocytes in different bones might create regional differences in the cellular composition of the HSC niche. We confirmed that perilipin[+] adipocytes were more abundant in caudal vertebrae than in femurs and tibias from normal young adult mice (compare Fig. 7a to 1n). The frequency of LepR^{+} stromal cells was significantly lower in bone marrow from caudal vertebrae as compared to femurs and tibia (Fig. 7b). $Adipoq$-Cre/ER recombined in $89\pm4.3\%$ of adipocytes (Fig. 7c, d) but only in $4.3\pm2.2\%$ of LepR^{+} stromal cells in caudal vertebrae (Fig. 7e).

Vascularization (Fig. 7g), endothelial cell frequency (Fig. 7h), LepR[+] cell frequency (Fig. 7i), total bone marrow cellularity (Fig. 7j), and HSC frequency (Fig. 7k) all progressively declined in distal (CA11-CA15) as compared to proximal (CA1–CA5) caudal vertebrae. To test whether HSCs depend upon SCF from adipocytes in these bones we treated 2-month-old $Adipoq$-$cre/ER; Scf^{GFP/fl}$ mice with tamoxifen. Four weeks later, $Adipoq$-$cre/ER; Scf^{GFP/fl}$ mice had significantly reduced total bone marrow cells (Fig. 7j) and HSCs (Fig. 7k) relative to control mice in all caudal vertebrae. The femurs and tibias of the same $Adipoq$-$cre/ER; Scf^{GFP/fl}$ mice did not show any hematopoietic defects. Bone marrow cells from middle

caudal vertebrae of *Adipoq-cre/ER; Scf^GFP/fl* mice gave significantly lower levels of donor cell reconstitution in all lineages as compared to control bone marrow cells (Fig. 7l). HSC maintenance thus depends upon SCF from adipocytes in caudal vertebrae, but not long bones, of non-irradiated young adult mice.

Positive and negative effects of adipocytes on regeneration in different bones

We ablated adipocytes by treating *Adipoq-cre/ER; R26^iDTR; R26^tdTomato* mice with tamoxifen and then diphtheria toxin. Diphtheria toxin initially eliminated most Tomato+ cells from the bone marrow but adipocytes were rapidly regenerated from unrecombined Tomato negative progenitors (presumably LepR+ cells) within 14 days (Supplementary Fig. 7i–k). This was not, therefore, an effective way to test whether adipocytes promote hematopoietic regeneration.

Instead, we examined A-ZIP/F1 mice, which constitutively inhibit the differentiation of adipocytes. As expected[29], these mice had modestly but significantly fewer adipocytes in their long bones (femurs+tibias; Fig. 8a) relative to littermate controls. In non-irradiated long bones, A-ZIP/F1 mice had normal numbers of bone marrow cells (Fig. 8b), HSCs (Fig. 8c), LSK cells (Fig. 8d), and LK cells (Fig. 8e). However, two weeks after irradiation, A-ZIP/F1 mice had significantly fewer total bone marrow cells (Fig. 8b), and LSK cells (Fig. 8d) as well as a trend toward reduced HSC numbers (p=0.057) in long bones as compared to control mice. In non-irradiated long bones, adipocytes are rare and are not a significant source of SCF but after irradiation they become abundant and promote regeneration.

Consistent with the results from Naveiras et al.[29], non-irradiated caudal vertebrae (CA6–CA10) from A-ZIP/F1 mice had substantially reduced numbers of adipocytes (Fig. 8h) accompanied by increased numbers of total bone marrow cells (Fig. 8i), HSCs (Fig. 8j), LSK cells (Fig. 8k), and LK cells (Fig. 8l) as compared to littermate controls. By 4 weeks after irradiation, A-ZIP/F1 mice had significantly increased numbers of total bone marrow cells (Fig. 8i), HSCs (Fig. 8j), LSK cells (Fig. 8k), and LK cells (Fig. 8l) in caudal vertebrae. Adipocytes therefore negatively regulate HSC frequency and hematopoietic regeneration in tail vertebrae.

In young adult long bones, the vasculature (Fig. 8o–q) and the numbers of LepR+ cells (Fig. 8f), and endothelial cells (Fig. 8g) appeared normal in non-irradiated A-ZIP/F1 mice and appeared to regenerate normally at 2 and 4 weeks after irradiation. In contrast, in non-irradiated caudal vertebra bone marrow, the vasculature was sparse relative to femur bone marrow (compare controls in Fig. 8r to 8o). With and without irradiation, caudal vertebrae in the A-ZIP/F1 mice had more sinusoidal blood vessels (Fig. 8r–t), LepR+ cells (Fig. 8m), and endothelial cells (Fig. 8n) as compared to littermate controls. This suggests that adipocytes negatively regulated the vascularization of the bone marrow in caudal vertebrae in a way that was not observed in long bones. The improved regeneration in the caudal vertebrae of A-ZIP/F1 mice correlated with increased vascularity. It is not clear whether this reflects only a developmental effect or whether there is an ongoing effect of adipocytes on the vasculature of caudal vertebrae in adult bone marrow. Overall, the data indicate that adipocytes promote HSC maintenance and hematopoietic regeneration by secreting SCF but that in adipocyte-

rich caudal vertebrae there is also an inhibition of bone marrow vascularization that has independent negative effects on HSC frequency and hematopoietic regeneration.

DISCUSSION

The long-standing clinical observation that adipocyte-rich yellow marrow is associated with reduced hematopoiesis in humans has commonly been interpreted to reflect a negative effect of adipocytes on hematopoiesis; however, our data suggest the opposite - that adipogenesis is an emergency response that promotes increased hematopoiesis in response to cytopenia. Adipogenesis is likely a faster way of increasing the production of HSC niche factors as compared to the construction of new perivascular niches, which would involve the generation of new blood vessels. Nonetheless, there are context-dependent differences in adipocyte function between bone marrow compartments (long bones versus caudal vertebrae) and there may also be differences between humans and mice.

When adipocytes have been co-cultured with hematopoietic cells, they have been reported to have a wide range of positive and negative effects on hematopoietic progenitors and hematopoiesis[50–53]. Beyond SCF, bone marrow adipocytes also synthesize adiponectin, which promotes HSC regeneration after irradiation by promoting HSC proliferation[54], as well as leptin[55], which promotes adipogenesis and inhibits osteogenesis by SSCs in the bone marrow[56]. Adipocytes likely secrete multiple factors that influence the function of HSCs and stromal cells in the bone marrow. Our results indicate that the sum of these effects promotes hematopoietic regeneration in most bones while inhibiting hematopoietic regeneration in caudal vertebrae.

METHODS

Mice

Mice were generally maintained on a C57BL/6 background, including *Lepr*[cre] [57], *Tie2-cre*[58], *Vav1-cre*[59], *Col1a1*2.3-cre*[43], *Adipoq-cre/ER*[45], *Scf*[GFP] [1], *Scf*^{fl/fl} [1], *R26*[tdTomato] [60], *R26*[iDTR] [61], *Fabp4-cre*[62] and *Col1a1*2.3-GFP*[63]. A-ZIP/F1 mice[34] were maintained on a FVB.C57BL/6 hybrid background. To induce CreER activity in *Adipoq*-Cre/ER mice, ~6 week-old mice were gavaged with 1 mg tamoxifen (Sigma, St. Louis, MO), dissolved in corn oil, daily for 3 consecutive days. To induce myeloablation by 5-FU, mice were intraperitoneally administered one or two doses of 5-FU (8 days apart; 150 mg/kg/day). All mice were housed in the Animal Resource Center at UT Southwestern Medical Center (UTSW) though some experiments were completed in the Animal Facility at the Shanghai Institute of Biochemistry and Cell Biology (SIBCB). All procedures were approved by the Institutional Animal Care and Use Committees of UTSW and SIBCB and all animal experiments were done in compliance with ethical guidelines and the approved protocols.

Human bone marrow specimens

Patient samples were collected during standard surgical procedures after obtaining written informed consent, approved by the Institutional Review Board of Texas Scottish Rite Hospital for Children (approval number IRB STU092011-034) and all experiments involving human samples were done in compliance with ethical guidelines and the approved

protocols. Bone marrow was harvested from the tibia (n=1) or femur (n=2) of pediatric patients (8 to 17 year-old) and transferred to cold PBS on ice.

Irradiation and hematopoietic regeneration

Adult mice were given two doses of 540 rads (total 1080 rads) at least 2 hours apart using an XRAD 320 x-ray irradiator (Precision X-Ray Inc., North Branford, CT). One million bone marrow cells from wild-type or *Ubc*-GFP mice were injected into the retro-orbital venus sinus of anaesthetized control or mutant mice for radioprotection. In most experiments recipient mice were maintained on antibiotic water (neomycin sulfate 1.11g/l and polymixin B 0.121g/l) for at least 14 days after transplantation, then switched to regular water.

Long-term competitive reconstitution assay

Adult recipient mice were irradiated using an XRAD 320 x-ray irradiator with two doses of 540 rad (total 1080 rad) delivered at least 2h apart. Cells were transplanted intravenously into the retro-orbital venous sinus of anesthetized mice. For competitive reconstitution assays we transplanted 3×10^5 donor bone marrow cells along with 3×10^5 recipient bone marrow cells. For secondary transplantation assays we transplanted 10^6 bone marrow cells from primary recipients along with 10^6 compromised (previously-transplanted, recipient-type) bone marrow cells. Mice were maintained on antibiotic water (neomycin sulfate 1.11g/l and polymixin B 0.121g/l) for 14 days then switched to regular water. Recipient mice were periodically bled to assess the level of donor-derived blood cells, including myeloid, B and T cells for 16 weeks after transplantation. Blood was subjected to ammonium chloride/potassium red cell lysis before antibody staining. Antibodies including anti-CD45.2 (104, 1:100), anti-CD45.1 (A20, 1:100), anti-Gr1 (8C5, 1:800), anti-Mac-1 (M1/70, 1:400), anti-B220 (6B2, 1:800), and anti-CD3 (KT31.1, 1:100) were used to stain cells for analysis by flow cytometry. All antibodies were obtained from eBioscience (San Diego, CA) or BD Bioscience (San Jose, CA).

Flow cytometry

Bone marrow cells were isolated by flushing the limb bones or by crushing the caudal vertebrae with a mortar and pestle in Ca^{2+} and Mg^{2+} free HBSS with 2% heat-inactivated bovine serum. For irradiated A-ZIP/F1 mice and their littermate controls, bone marrow cells from both limb bones and caudal vertebrae were isolated by crushing the bone. The cells were dissociated to a single cell suspension by passing through a 25G needle then filtering through a 40μm nylon mesh. The following antibodies were used to identify HSCs: anti-CD150 (TC15-12F12.2, 1:100), anti-CD48 (HM48-1, 1:100), anti-Sca1 (E13-161.7, 1:100), anti-c-kit (2B8, 1:100) and the following antibodies against lineage markers (anti-Ter119 (TER-119, 1:200), anti-B220, anti-Gr1, anti-CD2 (RM2-5, 1:200), anti-CD3, anti-CD5 (53–7.3, 1:400) and anti-CD8 (53–6.7, 1:400)). DAPI was used to exclude dead cells. Unless otherwise indicated, antibodies were obtained from eBioscience (San Diego, CA) or BD Bioscience (San Jose, CA).

For flow cytometric analysis of bone marrow stromal cells, bone marrow was gently flushed using HBSS with 2% bovine serum then digested with DNase I (200U/ml) and liberase[DL] (Roche, San Francisco, CA) at 37°C for 20 minutes. Samples were then stained with anti-

LepR (biotinylated, R&D Systems), anti-CD45 (30F-11), anti-CD31 (390), and anti-Ter119 antibodies to isolate stromal cells. For analysis of bone marrow endothelial cells, mice were i.v. injected with 10 μg/mouse Alexa Fluor 647 conjugated anti-VE-cadherin antibody (BV13, eBiosciences). Ten minutes later, the long bones were removed and bone marrow was flushed, digested and stained as above. Samples were analyzed using a FACSAria flow cytometer (BD Biosciences, San Jose, CA). Data were analyzed by FlowJo (Tree Star) software.

CFU-F assay and in vitro differentiation

For CFU-F assays with unfractionated bone marrow cells, freshly prepared single-cell suspensions were plated at a density of ~10^4 cells/cm^2 in 100-mm dishes in DMEM (Gibco) supplemented with 20% FBS qualified (Sigma), 10 μM Y-27632 (TOCRIS), and 1% penicillin/streptomycin (Invitrogen). For CFU-F assays with sorted cells, cells were sorted directly into culture at a density 10 cells/cm^2 in 6-well plates, ensuring that spatially distinct colonies would form at clonal density and therefore could be counted. The cultures were incubated at 37°C in a humidified, gas-tight chamber (Billups-Rothenberg, Del Mar, CA) with 5% O_2 and 10% CO_2 to enhance progenitor survival and proliferation[64]. CFU-F colonies were counted after 7–10 days of culture when they were distinguished from hematopoietic colonies (such as macrophage colonies) by staining with anti-CD45-APC. Adipocyte and osteoblastic differentiation were induced with STEMPRO® differentiation kits (Invitrogen) and detected by staining with Oil red O (Sigma) and Alizarin red S (Sigma), respectively[65]. For spontaneous differentiation, CFU-F colonies were maintained in DMEM plus 20% FBS for 1 week. Alkaline phosphatase staining was performed using the StemTAG™ Alkaline Phosphatase Staining and Activity Assay Kit (Cell Biolabs). Adipocytes were counted based on anti-perilipin staining.

Quantitative real-time PCR

Cells were sorted directly into Trizol (Life Technologies, Grand Island, NY). We isolated bone marrow adipocytes as described in a prior study[61], bone marrow from 6~8 month-old mice or recipient mice at 14 days after irradiation was digested as described above. Floating cells were transferred to a new tube, washed twice with HBSS and then transferred into Trizol. Total RNA was extracted according to the manufacturer's instructions. RNA was reverse transcribed using SuperScript III Reverse Transcriptase (Life Technologies). Quantitative real-time PCR was performed using SYBR green on a LightCycler 480 (Roche). *β-actin* was used to normalize the RNA content of samples. Primers used in this study were *Scf*: 5′-GCCAGAAACTAGATCCTTTACTCCTGA-3′ and 5′-CATAAATGGTTTTGTGACACTGACTCTG-3′; *Ob-Rb*: 5′-GATGTTCCAAACCCCAAGAA-3′ and 5′- TTCTGCATGCTTGGTAAAAAGA-3′; *leptin*: 5′-GTGGTGGCTGGTGTCAGAT-3′ and 5′-TTGATGAGGTGACCAAGGTG-3′; *perilipin*: 5′-GGCCTGGACGACAAAACC-3′ and 5′-CAGGATGGGCTCCATGAC-3′; *Adipoq*: 5′-TGTTCCTCTTAATCCTGCCCA -3′ and 5′-CCAACCTGCACAAGTTCCCTT-3′; *FABP4*: 5′-TTCGATGAAATCACC-3′ and 5′-GGTCGACTTTCCATC-3′; *β-actin*: 5′-GCTCTTTTCCAGCCTTCCTT-3′ and 5′-CTTCTGCATCCTGTCAGCAA-3′; human *Scf*: 5′-CCATTGATGCCTTCAAGGAC-3′

and 5′-GGCTGTCTCTTCTTCCAGTA-3′; human *Gapdh*: 5′-AAGGTCATCCCTGAGCTGAA-3′ and 5′-TGACAAAGTGGTCGTTGAGG-3′.

Bone sectioning, immunostaining, and confocal imaging

Freshly dissected bones were fixed in 4% paraformaldehyde overnight followed by 3-day decalcification in 10% EDTA. Bones were sectioned (5μm for thin sections and 50μm for thick sections) using the CryoJane tape-transfer system (Instrumedics, Ann Arbor, MI). Sections were blocked in PBS with 10% horse serum for 1 hour and then stained overnight with chicken-anti-GFP (Aves, Tigard, OR, 1:1000), anti-CD41-APC (eBioscience, eBioMWReg30, 1:200), goat-anti-c-kit (R&D, 1:400), rabbit-anti-perilipin (Sigma, 1:1000) and/or rabbit-anti-laminin (Abcam, Cambridge, MA, 1:400) antibodies. Donkey-anti-goat Alexa Fluor 647, donkey-anti-chicken Alexa Fluor 488 and/or Donkey-anti-goat Alexa Fluor 647 were used as secondary antibodies (Life Technologies, 1:400). Slides were mounted with anti-fade prolong gold (Life Technologies) and images were acquired with a Zeiss LSM780 confocal microscope.

Western-blot

Bone marrow was flushed out of the bone and then dissociated in 66% Trichoracetic acid (TCA) in water. Extracts were incubated on ice for at least 15 min and centrifuged at 16,100 × g at 4°C for 10 min. Precipitates were washed in acetone twice and the dried pellets were solubilized in 9M urea, 2% TritonX-100, and 1% DTT. Samples were separated on 4–12% Bis-Tris polyacrylamide gels (Invitrogen) and transferred to PVDF membrane (Millipore). The blots were incubated with primary antibodies overnight at 4°C and then with secondary antibodies. Blots were developed with the SuperSignal West Femtochemiluminescence kit (Thermo Scientific). Primary antibodies used: rabbit-anti-SCF (Abcam, catalogue number ab64677, 1:1000) and mouse-anti-Actin (Santa Cruz, clone AC-15, 1:20,000).

Statistics and Reproducibility

Panels generally represent multiple independent experiments performed on different days with different mice. Sample sizes were not pre-determined based on statistical power calculations. No formal randomization techniques were used but mice were allocated to experiments randomly and samples were processed in an arbitrary order. No blinding was performed. No animals were excluded from analyses. Variation was always indicated using standard deviation. For analysis of the statistical significance of differences between two groups we generally performed two-tailed Student's *t*-tests followed by Holm-Sidak's multiple comparisons tests. When samples were effectively matched, paired t-tests were used. For analysis of the statistical significance of differences among more than two groups, we performed one-way ANOVAs with Dunnett's multiple comparisons tests. When samples were effectively matched, we performed repeated measures one-way ANOVAs with the Geisser-Greenhouse method for sphericity corrections and Tukey's multiple comparisons tests. To assess the statistical significance of differences among multiple groups when the experimental design involved multiple conditions, such as time points or cell types in addition to differences in genotypes, we performed two-way ANOVAs with Sidak's multiple comparisons tests. When samples were effectively matched, we performed repeated measures two-way ANOVAs with Sidak's multiple comparisons tests. Normality was tested

using the Shapiro-Wilk tests or the D'Agostino-Pearson omnibus tests when sample sizes were sufficient. Most data were normally distributed. When they were not, data were log2-transformed prior to statistical testing. Variability within groups was tested using Levine's median test prior to performing t-tests or one-way ANOVAs. Other than in Figure 8, we rarely observed significant differences in variability within groups. When there were significant differences in variability within treatments, data were log2-transformed and tested again for normality and variability prior to statistical testing. For one-way repeated measures ANOVAs, sphericity was not assumed, it was corrected using the Geisser-Greenhouse method. To assess the statistical significance of differences in survival, we performed Gehan-Breslow-Wilcoxon tests. All statistical tests were performed using GraphPad with Prism7, following its Statistics Guide.

Data availability

Source data for Fig. 1k, 1l, 7b and Supplementary Fig. 3b–3f have been provided as Supplementary Table 1. All other data supporting the findings of this study are available from the corresponding author upon reasonable request.

Supplementary Material

Refer to Web version on PubMed Central for supplementary material.

Acknowledgments

References

1. Ding L, Saunders TL, Enikolopov G, Morrison SJ. Endothelial and perivascular cells maintain haematopoietic stem cells. Nature. 2012; 481:457–62. [PubMed: 22281595]

2. Ding L, Morrison SJ. Haematopoietic stem cells and early lymphoid progenitors occupy distinct bone marrow niches. Nature. 2013; 495:231–5. [PubMed: 23434755]

3. Acar M, et al. Deep imaging of bone marrow shows non-dividing stem cells are mainly perisinusoidal. Nature. 2015; 526:126–30. [PubMed: 26416744]

4. Zhou BO, Yue R, Murphy MM, Peyer JG, Morrison SJ. Leptin-receptor-expressing mesenchymal stromal cells represent the main source of bone formed by adult bone marrow. Cell Stem Cell. 2014; 15:154–68. [PubMed: 24953181]

5. Greenbaum A, et al. CXCL12 in early mesenchymal progenitors is required for haematopoietic stem-cell maintenance. Nature. 2013; 495:227–30. [PubMed: 23434756]

6. Oguro H, Ding L, Morrison SJ. SLAM family markers resolve functionally distinct subpopulations of hematopoietic stem cells and multipotent progenitors. Cell Stem Cell. 2013; 13:102–16. [PubMed: 23827712]

7. Sugiyama T, Kohara H, Noda M, Nagasawa T. Maintenance of the hematopoietic stem cell pool by CXCL12-CXCR4 chemokine signaling in bone marrow stromal cell niches. Immunity. 2006; 25:977–88. [PubMed: 17174120]

8. Omatsu Y, Seike M, Sugiyama T, Kume T, Nagasawa T. Foxc1 is a critical regulator of haematopoietic stem/progenitor cell niche formation. Nature. 2014; 508:536–40. [PubMed: 24590069]

9. Omatsu Y, et al. The essential functions of adipo-osteogenic progenitors as the hematopoietic stem and progenitor cell niche. Immunity. 2010; 33:387–99. [PubMed: 20850355]

10. Mendez-Ferrer S, et al. Mesenchymal and haematopoietic stem cells form a unique bone marrow niche. Nature. 2010; 466:829–34. [PubMed: 20703299]

11. Kunisaki Y, et al. Arteriolar niches maintain haematopoietic stem cell quiescence. Nature. 2013; 502:637–43. [PubMed: 24107994]

12. Morikawa S, et al. Prospective identification, isolation, and systemic transplantation of multipotent mesenchymal stem cells in murine bone marrow. J Exp Med. 2009; 206:2483–96. [PubMed: 19841085]

13. Sacchetti B, et al. Self-renewing osteoprogenitors in bone marrow sinusoids can organize a hematopoietic microenvironment. Cell. 2007; 131:324–36. [PubMed: 17956733]

14. Kfoury Y, Scadden DT. Mesenchymal cell contributions to the stem cell niche. Cell Stem Cell. 2015; 16:239–53. [PubMed: 25748931]

15. Mizoguchi T, et al. Osterix marks distinct waves of primitive and definitive stromal progenitors during bone marrow development. Dev Cell. 2014; 29:340–9. [PubMed: 24823377]

16. Rodeheffer MS, Birsoy K, Friedman JM. Identification of white adipocyte progenitor cells in vivo. Cell. 2008; 135:240–9. [PubMed: 18835024]

17. Festa E, et al. Adipocyte lineage cells contribute to the skin stem cell niche to drive hair cycling. Cell. 2011; 146:761–71. [PubMed: 21884937]

18. Lee P, et al. Irisin and FGF21 are cold-induced endocrine activators of brown fat function in humans. Cell Metab. 2014; 19:302–9. [PubMed: 24506871]

19. Park D, et al. Endogenous bone marrow MSCs are dynamic, fate-restricted participants in bone maintenance and regeneration. Cell Stem Cell. 2012; 10:259–72. [PubMed: 22385654]

20. Hanoun M, et al. Acute myelogenous leukemia-induced sympathetic neuropathy promotes malignancy in an altered hematopoietic stem cell niche. Cell Stem Cell. 2014; 15:365–75. [PubMed: 25017722]

21. Worthley DL, et al. Gremlin 1 identifies a skeletal stem cell with bone, cartilage, and reticular stromal potential. Cell. 2015; 160:269–84. [PubMed: 25594183]

22. Yamazaki S, et al. Nonmyelinating Schwann cells maintain hematopoietic stem cell hibernation in the bone marrow niche. Cell. 2011; 147:1146–58. [PubMed: 22118468]

23. Mendez-Ferrer S, Lucas D, Battista M, Frenette PS. Haematopoietic stem cell release is regulated by circadian oscillations. Nature. 2008; 452:442–7. [PubMed: 18256599]

24. Lucas D, et al. Chemotherapy-induced bone marrow nerve injury impairs hematopoietic regeneration. Nat Med. 2013; 19:695–703. [PubMed: 23644514]

25. Chow A, et al. Bone marrow CD169+ macrophages promote the retention of hematopoietic stem and progenitor cells in the mesenchymal stem cell niche. J Exp Med. 2011; 208:261–71. [PubMed: 21282381]

26. Christopher MJ, Rao M, Liu F, Woloszynek JR, Link DC. Expression of the G-CSF receptor in monocytic cells is sufficient to mediate hematopoietic progenitor mobilization by G-CSF in mice. J Exp Med. 2011; 208:251–60. [PubMed: 21282380]

27. Bruns I, et al. Megakaryocytes regulate hematopoietic stem cell quiescence through CXCL4 secretion. Nat Med. 2014; 20:1315–20. [PubMed: 25326802]

28. Zhao M, et al. Megakaryocytes maintain homeostatic quiescence and promote post-injury regeneration of hematopoietic stem cells. Nat Med. 2014; 20:1321–6. [PubMed: 25326798]

29. Naveiras O, et al. Bone-marrow adipocytes as negative regulators of the haematopoietic microenvironment. Nature. 2009; 460:259–63. [PubMed: 19516257]

30. Calvo W, Fliedner TM, Herbst E, Hugl E, Bruch C. Regeneration of blood-forming organs after autologous leukocyte transfusion in lethally irradiated dogs. II. Distribution and cellularity of the marrow in irradiated and transfused animals. Blood. 1976; 47:593–601. [PubMed: 1260123]

31. Meunier P, Aaron J, Edouard C, Vignon G. Osteoporosis and the replacement of cell populations of the marrow by adipose tissue. A quantitative study of 84 iliac bone biopsies. Clin Orthop Relat Res. 1971; 80:147–54. [PubMed: 5133320]

32. Abella E, et al. Bone marrow changes in anorexia nervosa are correlated with the amount of weight loss and not with other clinical findings. Am J Clin Pathol. 2002; 118:582–8. [PubMed: 12375646]

33. Gimble JM, Robinson CE, Wu X, Kelly KA. The function of adipocytes in the bone marrow stroma: an update. Bone. 1996; 19:421–8. [PubMed: 8922639]

34. Moitra J, et al. Life without white fat: a transgenic mouse. Genes Dev. 1998; 12:3168–81. [PubMed: 9784492]

35. Nunez NP, et al. Accelerated tumor formation in a fatless mouse with type 2 diabetes and inflammation. Cancer Res. 2006; 66:5469–76. [PubMed: 16707476]

36. Ablamunits V, et al. Susceptibility to induced and spontaneous carcinogenesis is increased in fatless A-ZIP/F-1 but not in obese ob/ob mice. Cancer Res. 2006; 66:8897–902. [PubMed: 16951207]

37. Hooper AT, et al. Engraftment and reconstitution of hematopoiesis is dependent on VEGFR2-mediated regeneration of sinusoidal endothelial cells. Cell Stem Cell. 2009; 4:263–74. [PubMed: 19265665]

38. Zhou BO, Ding L, Morrison SJ. Hematopoietic stem and progenitor cells regulate the regeneration of their niche by secreting Angiopoietin-1. Elife. 2015; 4:e05521. [PubMed: 25821987]

39. Kopp HG, et al. Tie2 activation contributes to hemangiogenic regeneration after myelosuppression. Blood. 2005; 106:505–13. [PubMed: 15817675]

40. Li XM, Hu Z, Jorgenson ML, Wingard JR, Slayton WB. Bone marrow sinusoidal endothelial cells undergo nonapoptotic cell death and are replaced by proliferating sinusoidal cells in situ to maintain the vascular niche following lethal irradiation. Exp Hematol. 2008; 36:1143–1156. [PubMed: 18718416]

41. Knospe WH, Blom J, Crosby WH. Regeneration of locally irradiated bone marrow. I. Dose dependent, long-term changes in the rat, with particular emphasis upon vascular and stromal reaction. Blood. 1966; 28:398–415. [PubMed: 5918471]

42. Greenberg AS, et al. Perilipin, a major hormonally regulated adipocyte-specific phosphoprotein associated with the periphery of lipid storage droplets. J Biol Chem. 1991; 266:11341–6. [PubMed: 2040638]

43. Liu F, et al. Expression and activity of osteoblast-targeted Cre recombinase transgenes in murine skeletal tissues. Int J Dev Biol. 2004; 48:645–53. [PubMed: 15470637]

44. Kiel MJ, et al. SLAM family receptors distinguish hematopoietic stem and progenitor cells and reveal endothelial niches for stem cells. Cell. 2005; 121:1109–21. [PubMed: 15989959]

45. Sassmann A, Offermanns S, Wettschureck N. Tamoxifen-inducible Cre-mediated recombination in adipocytes. Genesis. 2010; 48:618–25. [PubMed: 20715175]

46. Jeffery E, et al. Characterization of Cre recombinase models for the study of adipose tissue. Adipocyte. 2014; 3:206–11. [PubMed: 25068087]

47. Zhang CC, Lodish HF. Cytokines regulating hematopoietic stem cell function. Curr Opin Hematol. 2008; 15:307–11. [PubMed: 18536567]

48. Broudy VC. Stem cell factor and hematopoiesis. Blood. 1997; 90:1345–64. [PubMed: 9269751]

49. Randall TD, Weissman IL. Phenotypic and functional changes induced at the clonal level in hematopoietic stem cells after 5-fluorouracil treatment. Blood. 1997; 89:3596–606. [PubMed: 9160664]

50. Spindler TJ, Tseng AW, Zhou X, Adams GB. Adipocytic cells augment the support of primitive hematopoietic cells in vitro but have no effect in the bone marrow niche under homeostatic conditions. Stem Cells Dev. 2014; 23:434–41. [PubMed: 24083324]

51. Corre J, et al. Human bone marrow adipocytes support complete myeloid and lymphoid differentiation from human CD34 cells. Br J Haematol. 2004; 127:344–7. [PubMed: 15491297]

52. Glettig DL, Kaplan DL. Extending human hematopoietic stem cell survival in vitro with adipocytes. Biores Open Access. 2013; 2:179–85. [PubMed: 23741628]

53. Belaid-Choucair Z, et al. Human bone marrow adipocytes block granulopoiesis through neuropilin-1-induced granulocyte colony-stimulating factor inhibition. Stem Cells. 2008; 26:1556–64. [PubMed: 18388301]

54. DiMascio L, et al. Identification of adiponectin as a novel hemopoietic stem cell growth factor. J Immunol. 2007; 178:3511–20. [PubMed: 17339446]

55. Poloni A, et al. Molecular and functional characterization of human bone marrow adipocytes. Exp Hematol. 2013; 41:558–566 e2. [PubMed: 23435314]

56. Yue R, Zhou BO, Shimada IS, Zhao Z, Morrison SJ. Leptin Receptor Promotes Adipogenesis and Reduces Osteogenesis by Regulating Mesenchymal Stromal Cells in Adult Bone Marrow. Cell Stem Cell. 2016; 18:782–96. [PubMed: 27053299]

57. DeFalco J, et al. Virus-assisted mapping of neural inputs to a feeding center in the hypothalamus. Science. 2001; 291:2608–13. [PubMed: 11283374]

58. Koni PA, et al. Conditional vascular cell adhesion molecule 1 deletion in mice: impaired lymphocyte migration to bone marrow. J Exp Med. 2001; 193:741–54. [PubMed: 11257140]

59. de Boer J, et al. Transgenic mice with hematopoietic and lymphoid specific expression of Cre. Eur J Immunol. 2003; 33:314–25. [PubMed: 12548562]

60. Madisen L, et al. A robust and high-throughput Cre reporting and characterization system for the whole mouse brain. Nat Neurosci. 2010; 13:133–40. [PubMed: 20023653]

61. Buch T, et al. A Cre-inducible diphtheria toxin receptor mediates cell lineage ablation after toxin administration. Nat Methods. 2005; 2:419–26. [PubMed: 15908920]

62. He W, et al. Adipose-specific peroxisome proliferator-activated receptor gamma knockout causes insulin resistance in fat and liver but not in muscle. Proc Natl Acad Sci U S A. 2003; 100:15712–7. [PubMed: 14660788]

63. Kalajzic Z, et al. Directing the expression of a green fluorescent protein transgene in differentiated osteoblasts: comparison between rat type I collagen and rat osteocalcin promoters. Bone. 2002; 31:654–60. [PubMed: 12531558]

64. Morrison SJ, et al. Transient Notch activation initiates an irreversible switch from neurogenesis to gliogenesis by neural crest stem cells. Cell. 2000; 101:499–510. [PubMed: 10850492]

65. Bianco P, Kuznetsov SA, Riminucci M, Gehron Robey P. Postnatal skeletal stem cells. Methods Enzymol. 2006; 419:117–48. [PubMed: 17141054]
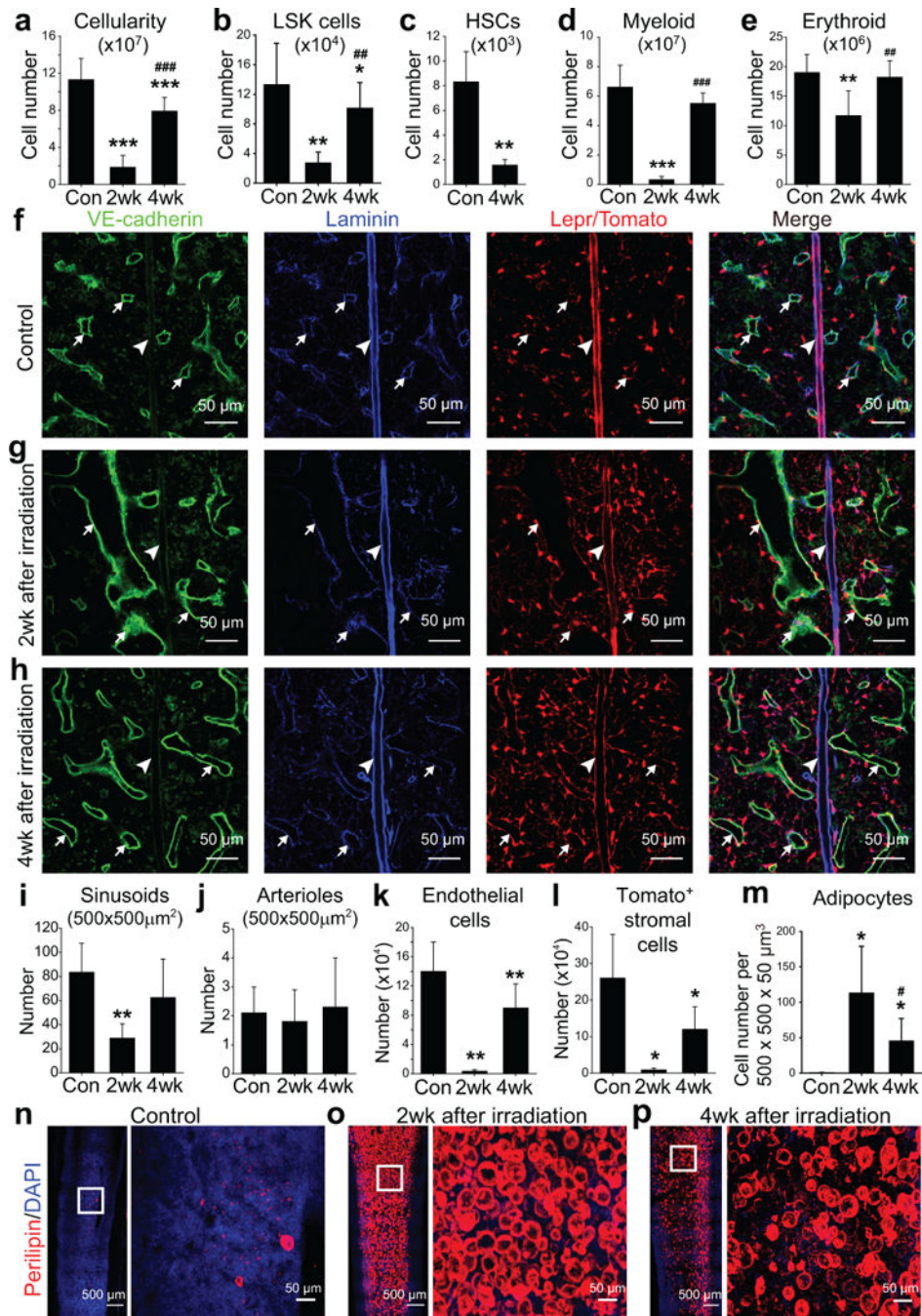
Figure 1. Irradiation disrupted sinusoids and depleted HSCs, endothelial cells, and LepR$^+$ stromal cells while dramatically increasing adipocytes in the bone marrow

One million bone marrow cells from wild-type mice were transplanted into irradiated wild-type (a–e and m–p) or *Lepr^{cre}; R26^{tdTomato}* (f–l) mice. Statistical significance was assessed using repeated measures one-way ANOVAs with Geisser-Greenhouse sphericity corrections along with Tukey's multiple comparisons tests (a–e, i–m). * indicates statistical significance relative to control (Con) while # indicates statistical significance of differences between 2 and 4 weeks after irradiation (* or # P<0.05, ** or ## P<0.01, *** or ### P<0.001). All data represent mean±SD.

(a–e) Flow cytometric analysis of mechanically dissociated bone marrow cells revealed significant reductions in bone marrow cellularity (a) and the numbers of Lineage$^-$Sca-1$^+$c-kit$^+$ (LSK) cells (b), CD150$^+$CD48$^-$Lineage$^-$Sca-1$^+$c-kit$^+$ HSCs (c), Mac1$^+$Gr-1$^+$ myeloid cells (d) and Ter119$^+$ erythroid cells (e) at 2 and/or 4 weeks after irradiation as compared to non-irradiated control mice. Cell numbers reflect two femurs and two tibias per mouse (n=5 mice/treatment from 5 independent experiments).

(f–h) Confocal imaging of thin femur sections from non-irradiated *Lepr*^{cre}; *R26*^{tdTomato} mice (control, f) or at 2 weeks (g) or 4 weeks (h) after irradiation and bone marrow transplantation. Arrows indicate sinusoidal blood vessels and arrowheads indicate arterioles.

(i, j) The densities of VE-cadhern^{bright}laminin^{dim} sinusoids (i) and VE-cadherin^{dim}laminin^{bright} arterioles (j) were quantified in sections (n=5 mice/condition from 3 independent experiments).

(k, l) Flow cytometric analysis of enzymatically dissociated bone marrow cells from *Lepr*^{cre}; *R26*^{tdTomato} mice revealed significant reductions in the numbers of VE-cadherin$^+$ endothelial cells (k) and Tomato$^+$ stromal cells (l) after irradiation (n=4 mice/condition from 4 independent experiments).

(m) Adipocyte numbers in thick femur sections from non-irradiated mice (Con) or mice at 2 or 4 weeks after irradiation (n=6 mice/condition from 3 independent experiments).

(n–p) Whole-mount imaging of thick femur sections (50-μm) from non-irradiated mice (Control, n) or mice 2 (o) or 4 (p) weeks after irradiation and bone marrow transplantation. Adipocytes were identified based on anti-perilipin staining (n=6 mice/condition from 3 independent experiments).
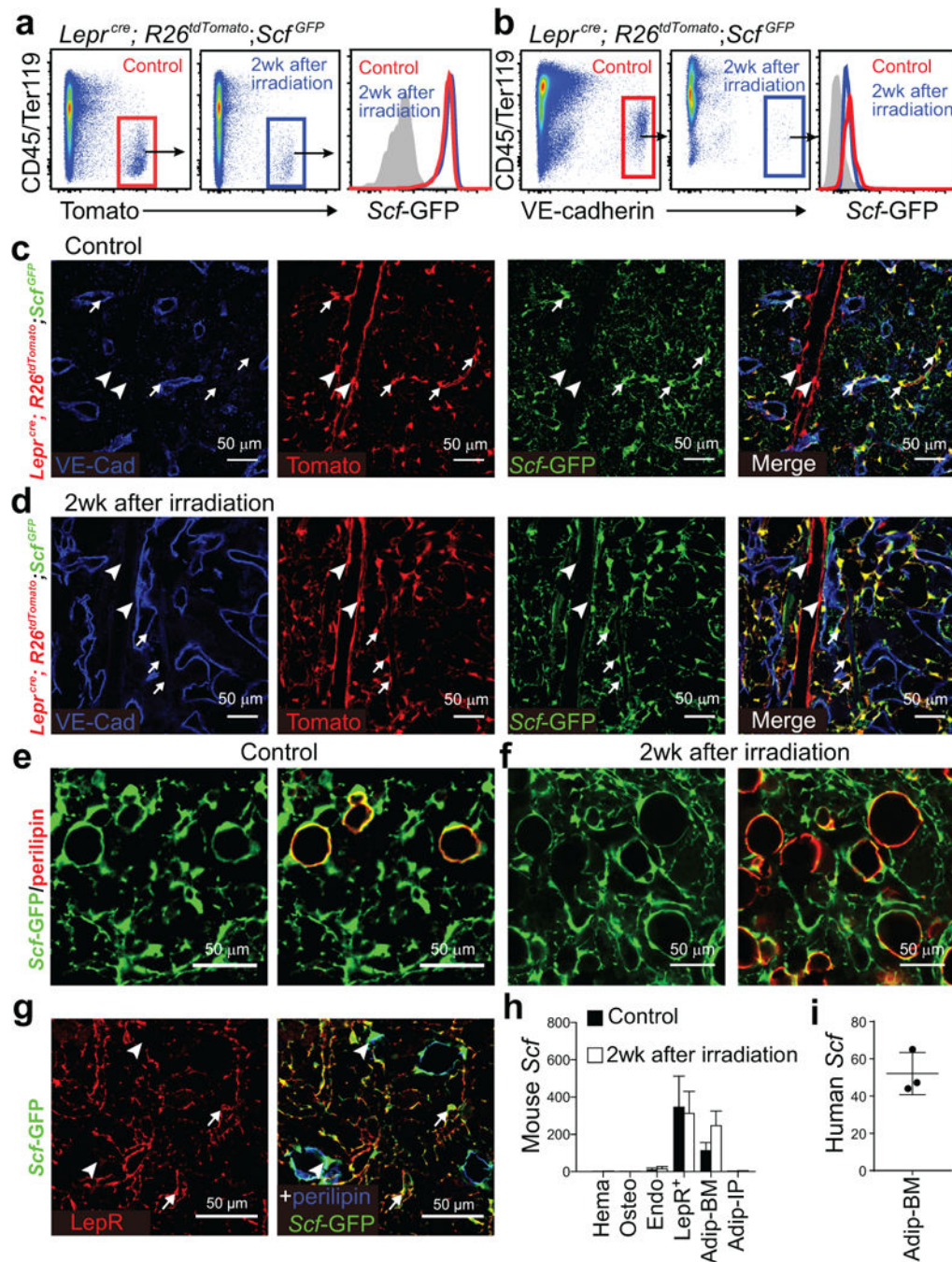
Figure 2. *Scf* was highly expressed by LepR^{+} stromal cells and adipocytes in the bone marrow before and after irradiation

One million whole bone marrow cells from wild-type mice were transplanted into irradiated *Lepr*[cre]; *R26*[tdTomato]; *Scf*[GFP] (a-d) or *Scf*[GFP] (e, f) mice.

(a, b) Flow cytometric analysis of enzymatically dissociated bone marrow cells from *Lepr*[cre]; *R26*[tdTomato]; *Scf*[GFP] mice showed that *Scf*-GFP was expressed at a high level by LepR^{+} stromal cells (a) and at a low level by endothelial cells (b) in non-irradiated mice (Control) and at 2 weeks after irradiation and bone marrow transplantation (representative results from 3 independent experiments).

(c, d) Representative femur diaphysis sections showed *Scf*-GFP expression by Tomato^{+} stromal cells in the bone marrow of *Lepr^{cre}; R26^{tdTomato}; Scf^{GFP}* mice that were not irradiated (Control, c) or at 2 weeks after irradiation and bone marrow transplantation (d). Tomato^{+} cells around small arterioles and sinusoids (arrows) expressed *Scf*-GFP while Tomato^{+} cells around large arterioles (arrowheads) did not (representative results from 3 independent experiments).

(e, f) Representative femur metaphysis sections showed *Scf*-GFP expression by perilipin[+] adipocytes in non-irradiated mice (Control, e) and at 2 weeks after irradiation and bone marrow transplantation (f) (representative results from 6 independent experiments). Note that the subcellular distribution of perilipin and GFP differ. See Supplementary Fig. 2e for serial optical sections showing *Scf*-GFP expression by a periliplin[+] adipocyte.

(g) Confocal imaging of thin femur sections from non-irradiated *Scf^{GFP}* mice co-stained with anti-LepR and anti-perilipin antibodies. LepR^{+} cells were *Scf*-GFP[+] but perilipin negative (arrows). Perilipin^{+} cells were *Scf*-GFP[+] but LepR negative (arrowheads; representative results from 3 independent experiments).

(h, i) Quantitative RT-PCR analysis of *Scf* transcript levels (normalized to β-*Actin*) in CD45^{+}/Ter119^{+} hematopoietic cells (Hema), *Col1a1*2.3*-GFP^{+} osteoblasts (Osteo), VE-cadherin^{+} endothelial cells (Endo), Tomato^{+}CD45^{−}Ter119^{−} bone marrow stromal cells from *Lepr^{cre}; R26^{tdTomato}* mice (LepR^{+}), bone marrow adipocytes (Adip-BM) and intraperitoneal adipocytes (Adip-IP) relative to unfractionated bone marrow cells in mouse (h) and human bone marrow (i). The *Scf* transcript level in unfractionated bone marrow cells was normalized to 1. Data represent mean±SD (n=3 mice (h) and n=3 human (i) samples, each from 3 independent experiments).
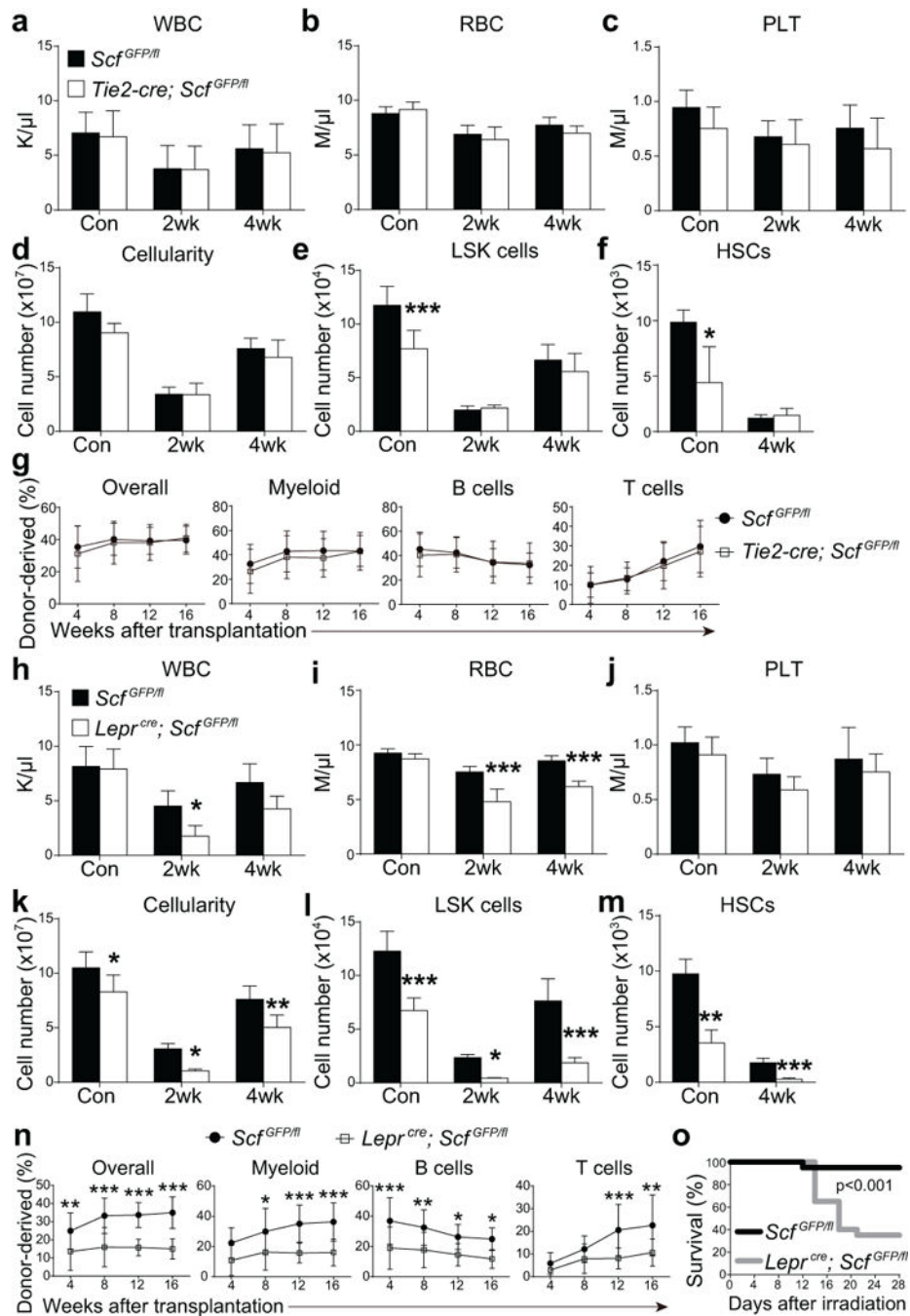
Figure 3. Scf from LepR+ stromal cells, but not endothelial cells, is necessary for hematopoietic regeneration and mouse survival after irradiation

(a–f) White blood cell (a) red blood cell (b), and platelet counts (c), as well as bone marrow (two femurs and two tibias per mouse) cellularity (d) and numbers of Lineage−Sca-1+c-kit+ cells (e) and CD150+CD48−Lineage−Sca-1+c-kit+ HSCs (f) from paired *Tie2-cre; Scf^GFP/fl* mice and *Scf^GFP/fl* controls that were non-irradiated (Con) or analyzed 2 or 4 weeks after irradiation and bone marrow transplantation. n=5 mice/genotype/condition from 3 independent experiments. HSCs could not be detected at 2 weeks after irradiation. Two-way ANOVAs with Sidak's multiple comparisons tests (a-e) or two-tailed Student's t-tests with

Holm-Sidak's multiple comparisons test (f) were used to assess differences between *Tie2-cre; Scf^{GFP/fl}* and *Scf^{GFP/fl}* mice.

(g) 10^6 donor bone marrow cells from the indicated primary recipient mice were transplanted 4 weeks after irradiation along with recipient-type competitor cells into irradiated secondary recipient mice (n=12 recipient mice/genotype from 3 independent experiments). Differences were assessed using two-way ANOVAs with Sidak's multiple comparisons tests.

(h–m) White blood cell (h) red blood cell (i), and platelet counts (j), as well as bone marrow cellularity (k) and numbers of LSK cells (l) and HSCs (m) from paired *Lepr-cre; Scf^{GFP/fl}* mice and *Scf^{GFP/fl}* controls that were non-irradiated (Con) or analyzed at 2 or 4 weeks after irradiation and bone marrow transplantation (n=5 mice/genotype/condition from 3 independent experiments). Two-way ANOVAs with Sidak's multiple comparisons tests (h-l) or two-tailed Student's t-tests with Holm-Sidak's multiple comparisons test (m) were used to assess the statistical significance of differences between *Lepr-cre; Scf^{GFP/fl}* and *Scf^{GFP/fl}* mice.

(n) 10^6 donor bone marrow cells from the indicated primary recipient mice were transplanted 4 weeks after irradiation along with recipient competitor cells into irradiated secondary recipient mice (n=12 recipient mice/genotype from 3 independent experiments). Differences were assessed using two-way ANOVAs with Sidak's multiple comparisons test (*P<0.05, **P<0.01, ***P<0.001).

(o) Mouse survival after irradiation and transplantation of 2×10^5 whole bone marrow cells (n=20 mice/genotype/condition from 5 independent experiments). The Gehan-Breslow-Wilcoxon test was used to assess statistical significance.

All data in Figure 3 represent mean±SD.
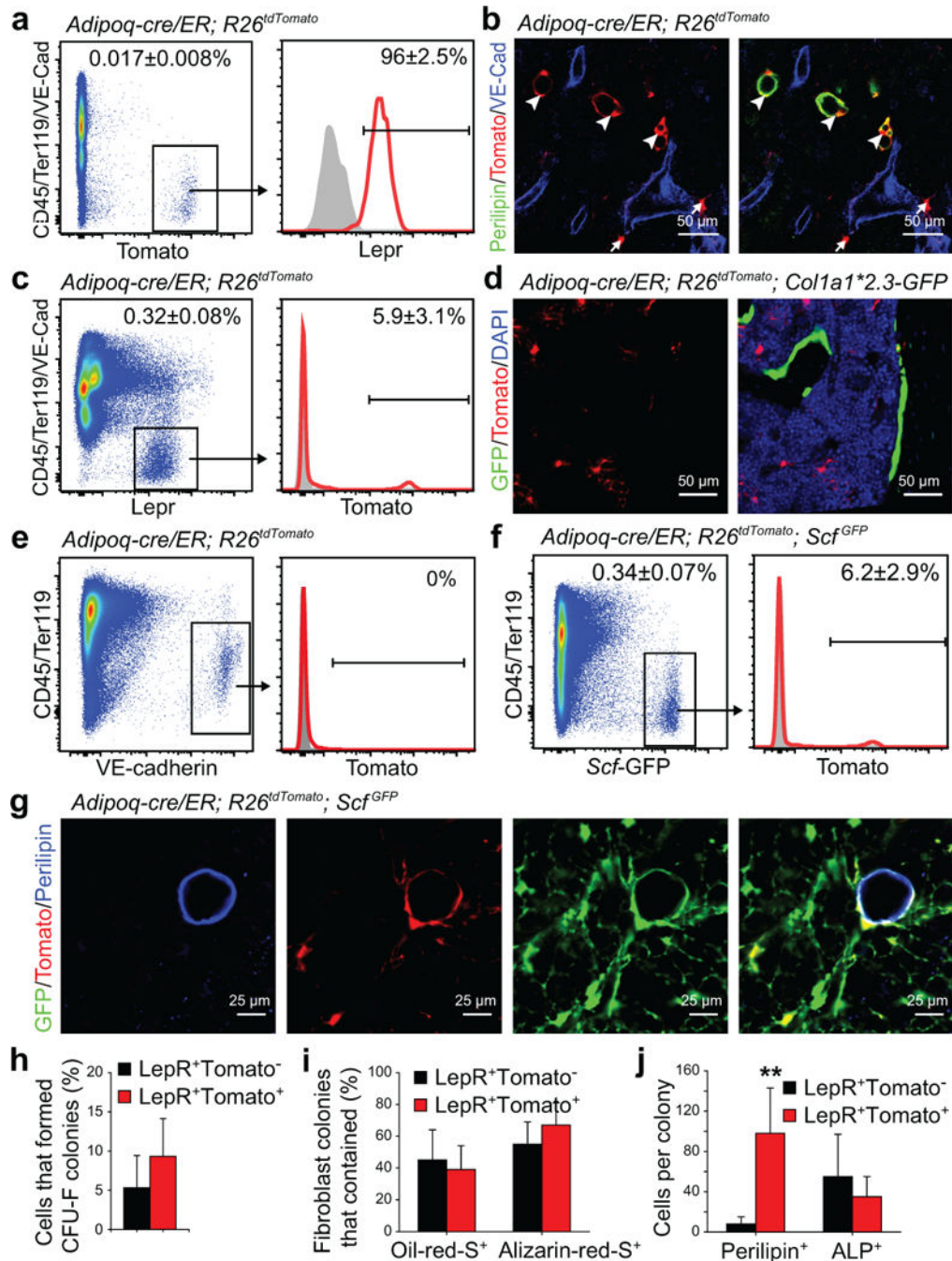
Figure 4. *Adipoq*-Cre/ER recombines in most adipocytes and in a subset of LepR^{+} stromal cells in the bone marrow

(a) 0.017±0.008% of bone marrow cells were Tomato[+] in enzymatically dissociated bone marrow cells from *Adipoq-cre/ER; R26[tdTomato]* mice at 4 weeks after tamoxifen administration.

(b) *Adipoq-cre/ER; R26[tdTomato]* mice exhibited Tomato expression by perilipin[+] adipocytes (arrowheads) and a subset of perilipin negative stromal cells (arrows) in the bone marrow.

(c) Only 5.9±3.1% of LepR^{+} stromal cells were Tomato[+] in the bone marrow of *Adipoq-cre/ER; R26[tdTomato]* mice at 4 weeks after tamoxifen administration.

(d) Tomato expression was rarely detected in bone-lining GFP$^+$ osteoblasts from *Adipoq-cre/ER; R26^{tdTomato}; Col1a1*2.3-GFP* mice.

(e) Tomato expression was not detected in VE-cadherin$^+$CD45/Ter119$^-$ endothelial cells in the bone marrow of *Adipoq-cre/ER; R26^{tdTomato}* mice at 4 weeks after tamoxifen administration.

(f) Only 6.2±2.9% of *Scf*-GFP$^+$ stromal cells were Tomato$^+$ in the bone marrow of *Adipoq-cre/ER; R26^{tdTomato}; Scf^{GFP}* mice at 4 weeks after tamoxifen administration.

(g) While not detected by flow cytometry, perilipin$^+$ adipocytes in bone marrow sections from *Adipoq-cre/ER; R26^{tdTomato}; Scf^{GFP}* mice were consistently positive for *Scf*-GFP and Tomato.

(h) Percentages of LepR$^+$Tomato$^-$ or LepR$^+$Tomato$^+$ stromal cells from *Adipoq-cre/ER; R26^{tdTomato}* mice that formed CFU-F colonies in culture.

(i) Percentage of CFU-F colonies that contained Oil-red-O$^+$ adipocytes or Alzarin-red-S$^+$ osteoblastic cells.

(j) The average numbers of perilipin$^+$ adipocytes or alkaline phosphatase$^+$ (ALP$^+$) osteogenic cells that spontaneously differentiated per CFU-F colony after 1 week of culture in DMEM plus 20% FBS (n=53 colonies from 3 mice; 3 independent experiments). A two-way ANOVA with Sidak's multiple comparisons test was used to assess statistical significance. **$P<0.01$.

All data in Figure 4 represent mean±SD and representative images from n=3 mice in 3 independent experiments.
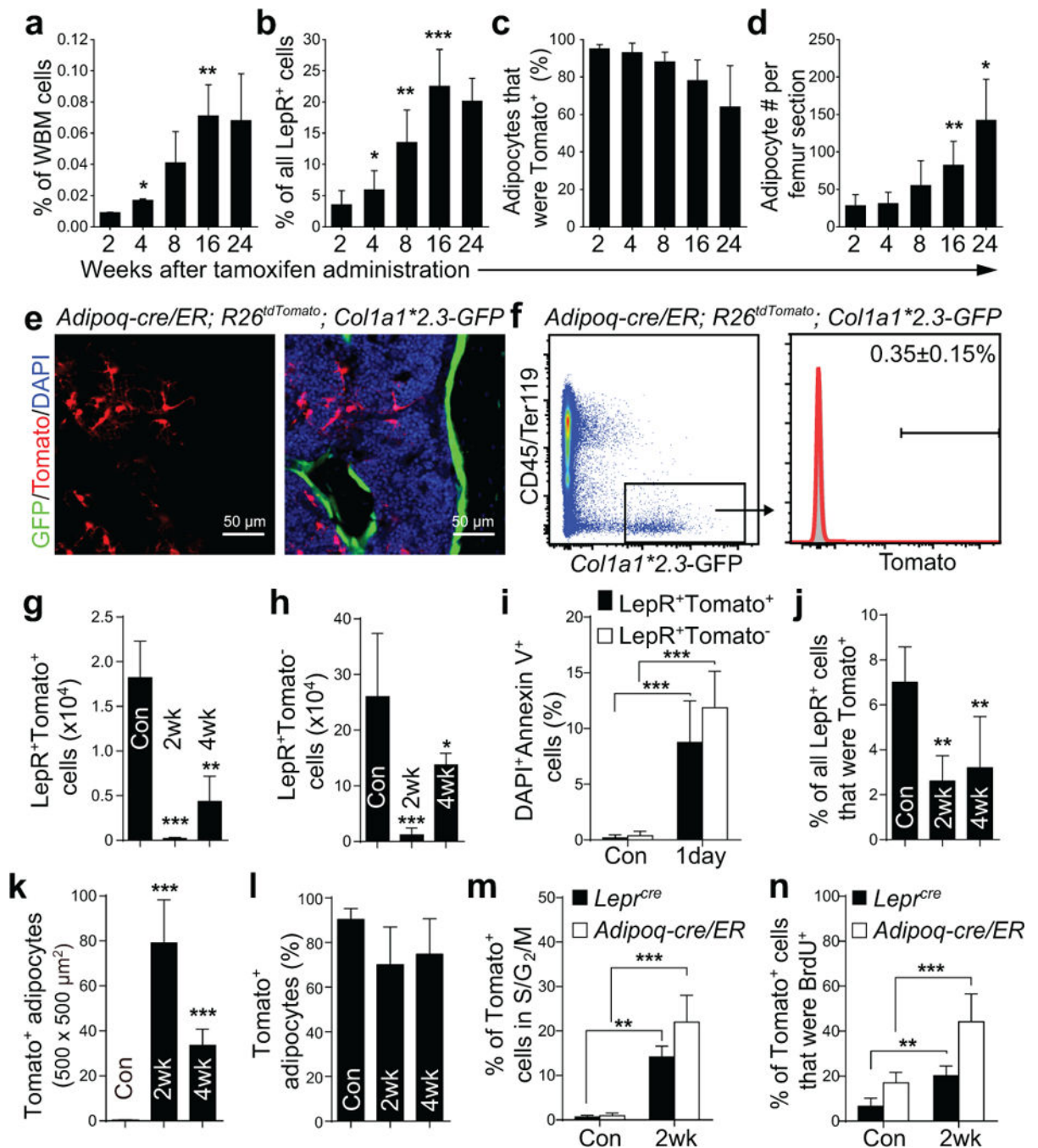
Figure 5. *Adipoq*-Cre/ER[+] bone marrow stromal cells form adipocytes, but rarely osteoblasts, in vivo

(a–d) Percentages of whole bone marrow (WBM) cells (a; by flow cytometry), LepR^{+} stromal cells (b; by flow cytometry), or adipocytes (c; by microscopy in sections) that were Tomato[+] in *Adipoq-cre/ER; R26[tdTomato]* mice at 2–24 weeks after tamoxifen administration. Numbers of adipocytes/section (d). Two-way ANOVAs with Sidak's multiple comparisons tests were used to assess differences among consecutive ages (*P<0.05, **P<0.01, ***P<0.001).

(e, f) Four months after tamoxifen treatment, *Adipoq-cre/ER; R26^{tdTomato}; Col1a1*2.3-GFP* mice had only rare GFP$^+$ osteoblasts that were Tomato$^+$ in bone marrow sections (e) or by flow cytometry (f).

(g, h) Based on flow cytometric analysis, the numbers of LepR$^+$Tomato$^+$ cells (g) and LepR$^+$Tomato$^-$ cells (h) declined in *Adipoq-cre/ER; R26^{tdTomato}* mice after irradiation and bone marrow transplantation. Differences between non-irradiated (Con) and irradiated mice (at 2 or 4 weeks) were assessed by one-way ANOVAs with Dunnett's multiple comparisons tests (data from panel g were log2-transformed) (**p<0.01, ***P<0.001).

(i) Percentages of LepR$^+$Tomato$^+$ or LepR$^+$Tomato$^-$ cells that were also DAPI$^+$Annexin V$^+$ in enzymatically dissociated bone marrow cells from *Adipoq-cre/ER; R26^{tdTomato}* mice one day after irradiation. A two-way ANOVA with Sidak's multiple comparisons test was used to assess differences among treatments.

(j, k) The percentages of LepR$^+$ cells that were Tomato$^+$ (j) declined in *Adipoq-cre/ER; R26^{tdTomato}* mice after irradiation. In contrast, the number of Tomato$^+$ adipocytes in femur sections increased after irradiation (k). The statistical significance of differences between non-irradiated (Con) and irradiated mice was measured using one-way ANOVAs with Dunnett's multiple comparisons tests (data of 5k were log2-transformed) (**P<0.01, ***P<0.001).

(l) The vast majority of bone marrow adipocytes were Tomato$^+$ in non-irradiated and irradiated *Adipoq-cre/ER; R26^{tdTomato}* mice.

(m, n) Hoechst staining (m) and BrdU incorporation (14 day pulse, n) by Tomato$^+$ bone marrow stromal cells in *Adipoq-cre/ER; R26^{tdTomato}* mice or *Lepr^{cre}; R26^{tdTomato}* mice that were non-irradiated (Con) or at 2 weeks after irradiation and bone marrow transplantation. Two-way repeated measures ANOVAs with Sidak's multiple comparisons tests was used to assess differences among treatments.

All data in Figure 5 represent mean±SD from n=5 mice/time point from 3 independent experiments.
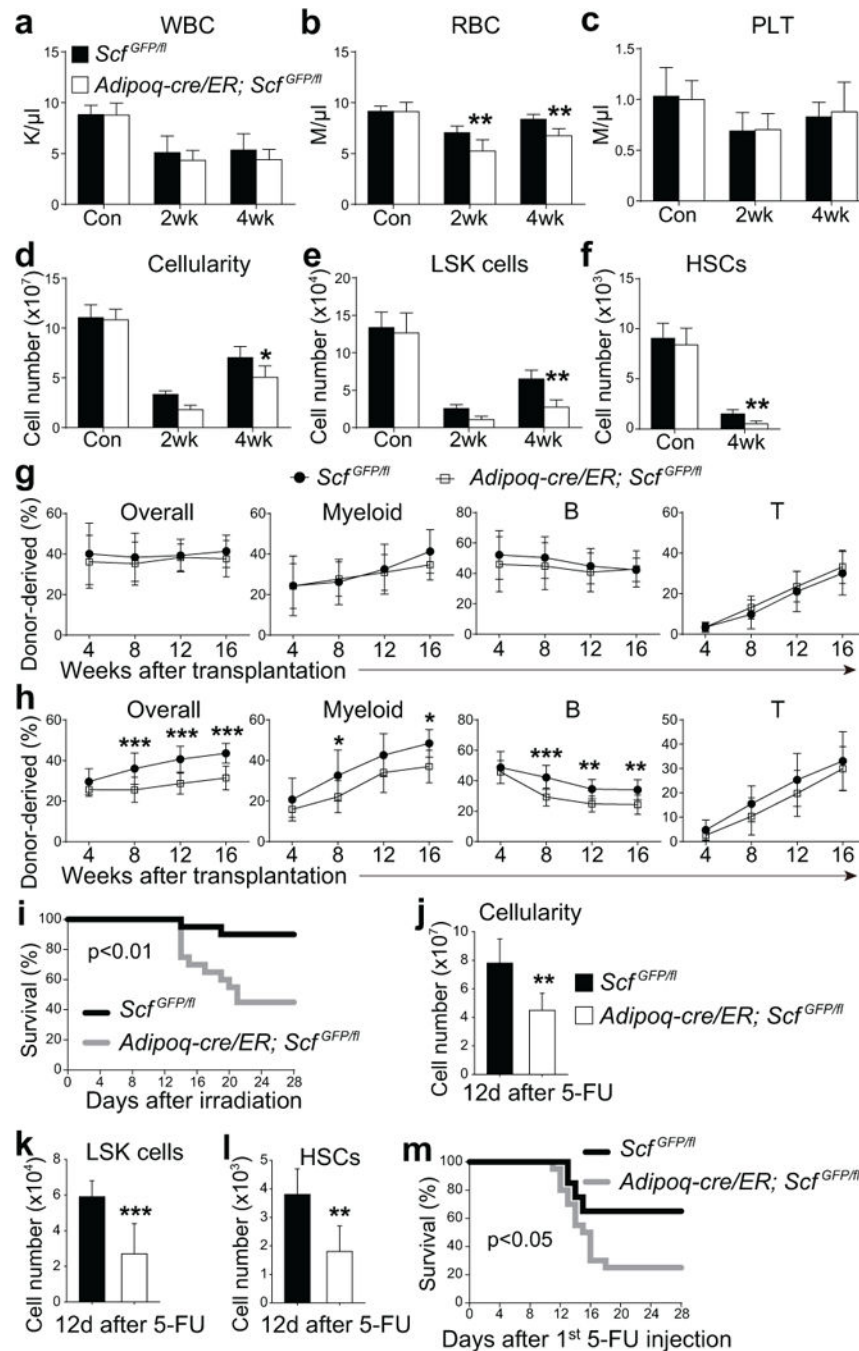
Figure 6. *Scf* from adipocytes is required for the regeneration of HSCs and hematopoiesis and mouse survival after irradiation

(a–i) One million WBM cells were transplanted into irradiated *Adipoq-cre/ER; Scf^GFP/fl* mice or Scf^GFP/fl^ controls 2 weeks after tamoxifen treatment. Non-irradiated *Adipoq-cre/ER; Scf^GFP/fl* mice and Scf^GFP/fl^ controls mice were treated with tamoxifen 4 weeks before analysis.

(a–f) White blood cell (a) red blood cell (b), and platelet counts (c), as well as WBM cellularity (d) and numbers of LSK cells (e) and HSCs (f) from *Adipoq-cre/ER; Scf^GFP/fl* and *Scf^GFP/fl* mice that were non-irradiated (Con) or analyzed at 2 or 4 weeks after

irradiation and bone marrow transplantation. n=5 mice/genotype/condition from 3 independent experiments from two femurs and two tibias per mouse. HSCs could not be detected 2 weeks after irradiation. Two-way ANOVAs with Sidak's multiple comparisons tests (a–e) or two-tailed Student's t-tests with Holm-Sidak's multiple comparisons test (f) were used to assess differences between *Adipoq-cre/ER; Scf$^{GFP/fl}$* and *Scf$^{GFP/fl}$* mice (*P<0.05, **P<0.01).

(g) 3×10^5 donor WBM cells from the femurs and tibias of non-irradiated mice were transplanted along with equal numbers of recipient WBM cells into irradiated recipient mice. (n=12 recipient mice/genotype from 3 independent experiments). Statistical significance was assessed using two-way repeated measures ANOVAs.

(h) 10^6 donor WBM cells from the indicated primary recipient mice were transplanted 4 weeks after irradiation along with equal numbers of recipient WBM cells into irradiated secondary recipient mice (n=12 recipient mice/genotype from 3 independent experiments). Statistical significance was assessed using two-way repeated measures ANOVAs with Sidak's multiple comparisons tests (*P<0.05, **P<0.01, ***P<0.001).

(i) Mouse survival after irradiation and transplantation of 10^5 WBM cells (n=20 mice/genotype).

(j–l) WBM cellularity (j) and numbers of LSK cells (k) and HSCs (l) from paired *Adipoq-cre/ER; Scf$^{GFP/fl}$* mice and *Scf$^{GFP/fl}$* controls 12 days after 5-FU treatment (*P<0.05; n=7 mice/genotype). Differences between genotypes were assessed using two-tailed Student's t-tests.

(m) Survival of *Adipoq-cre/ER; Scf$^{GFP/fl}$* mice and *Scf$^{GFP/fl}$* controls after two doses of 5-FU (on days 1 and 8; n=20 mice/genotype). A Gehan-Breslow-Wilcoxon test was used to assess statistical significance in panels i and m. All data in Figure 6 represent mean±SD.
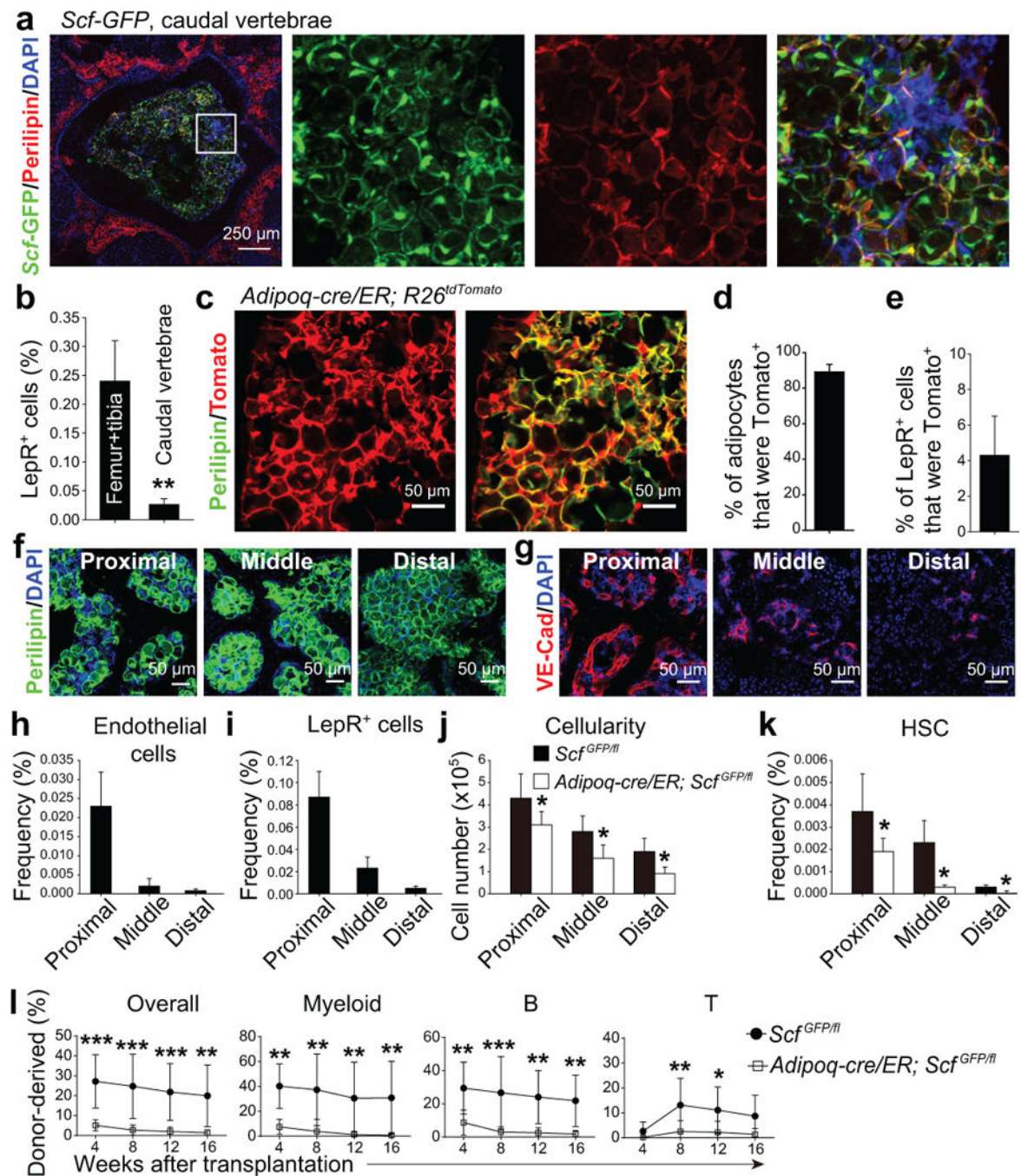
Figure 7. *Scf* from adipocytes is required for normal HSC frequency and hematopoiesis in the caudal vertebrae of normal young adult mice

(a) Whole-mount imaging of cross sections of a caudal vertebra showing large numbers of adipocytes in the bone marrow (representative image from 3 independent experiments performed on CA1-CA5 vertebrae).

(b) The frequency of LepR+ stromal cells in bone marrow from femurs and tibia versus caudal vertebrae (CA1-CA5). Data represent mean±SD from n=3 mice in 3 independent experiments. A two-tailed Student's t-test was used to assess the statistical significance between genotypes (data were log2-transformed; **P<0.01).

(c–e) *Adipoq*-Cre/ER recombined in nearly all adipocytes (c, d) but only in a small subset of LepR$^+$ stromal cells (e) four weeks after tamoxifen treatment. Data represent mean±SD from n=3 mice in 3 independent experiments.

(f) Adipocytes were abundant in all caudal vertebrae (proximal=CA1-CA5; middle=CA6-CA10; distal=CA11-CA16; representative images from 3 independent experiments).

(g) Bone marrow vascularity progressively declined in caudal vertebrae (representative images from 3 independent experiments).

(h–k) Endothelial cell frequency (h), LepR$^+$ cell frequency (i), total bone marrow cellularity (j), and HSC frequency (k) in caudal vertebrae from *Adipoq-cre/ER; Scf$^{GFP/fl}$* mice and *Scf$^{GFP/fl}$* controls that had been administered tamoxifen 4 weeks earlier. Data represent mean±SD from n=5 mice/treatment in 3 independent experiments. Paired, two-tailed Student's t-tests with Holm-Sidak's multiple comparisons tests were used to assess statistical significance for j and k (*P<0.05).

(l) Competitive reconstitution assay in which 5×10^5 donor bone marrow cells from middle caudal vertebrae were transplanted along with equal numbers of recipient bone marrow cells into irradiated recipient mice. All data represent mean±SD (n=10 recipient mice/genotype from 3 independent experiments). The statistical significance of differences was assessed using two-way ANOVAs with Sidak's multiple comparisons tests (*P<0.05, **P<0.01, ***P<0.001).
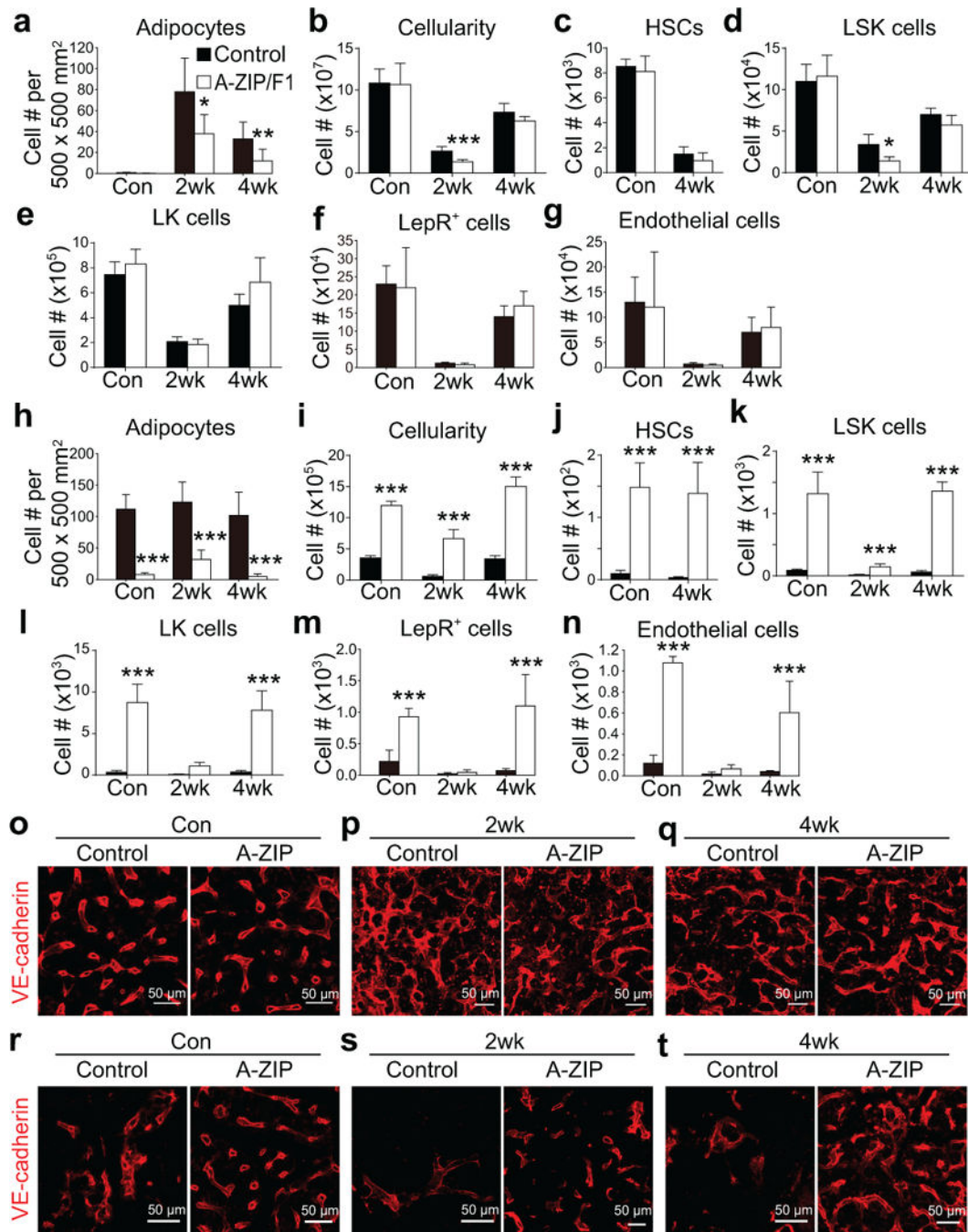
Figure 8. A-ZIP/F1 'fatless' mice exhibit delayed hematopoietic regeneration in the femur but accelerated regeneration of hematopoiesis and vasculature in caudal vertebrae

All data in panels a-n represent mean±SD from n=5 mice (con and 4wk) or n=8 mice (2wk)/ genotype/treatment from 3 independent experiments performed on leg bones (femurs+tibia; a–g) or caudal vertebrae (CA6-CA10, h-n) from non-irradiated control mice (con) or mice at 2 or 4 weeks after irradiation and bone marrow transplantation. Two-way ANOVAs (b–e) or repeated measures two-way ANOVAs (a and f-n) with Sidak's multiple comparisons tests were used to assess the statistical significance of differences between control and A-ZIP/F1 mice (*P<0.05, **P<0.01, ***P<0.001). Data in some panels (a, b, e, and j–n) were log2-

transformed prior to performing these statistical tests because the data showed unequal variance among groups.

(a) Perilipin$^+$ adipocytes in thin femur sections.

(b–g) Numbers of total bone marrow cells (b), HSCs (c), LSK cells (d), LK cells (e), LepR$^+$ stromal cells (f) and VE-cadherin$^+$ endothelial cells (g) in two femurs and two tibias.

(h) Perilipin$^+$ adipocytes in thin caudal vertebra sections.

(i–n) Numbers of total bone marrow cells (i), HSCs (j), LSK cells (k), LK cells (l), LepR$^+$ stromal cells (m) and VE-cadherin$^+$ endothelial cells (n) per caudal vertebra.

(o–q) Confocal imaging of thin femur sections from control and A-ZIP/F1 mice that were non-irradiated (Con) or analyzed at 2 or 4 weeks after irradiation and bone marrow transplantation. (images are representative of 3 mice/genotype/condition from 3 independent experiments).

(r–t) Confocal imaging of thin caudal vertebra sections from control and A-ZIP/F1 mice that were non-irradiated (Con) or analyzed at 2 or 4 weeks after irradiation and bone marrow transplantation. (n=3 mice/genotype/condition from 3 independent experiments).